UNIVERSIDADE DA BEIRA INTERIOR
Ciências

Assess of catechol-*O*-methyltransferase soluble isoform by multiple reaction monitoring mass spectrometry

Joana Margarida Santos Diogo

Dissertação para obtenção do Grau de Mestre em

Bioquímica

(2º ciclo de estudos)

Orientador: Prof. Doutor Luís António Paulino Passarinha

Co-Orientador: Profª. Doutora María Eugénia Gallardo Alba

Covilhã, outubro de 2016

Somewhere, something incredible is waiting to be known.

Carl Sagan

1. Acknowledgments

Em primeiro lugar, gostaria de agradecer ao professor Doutor Luís António Paulino Passarinha e à professora Doutora María Eugénia Gallardo Alba, por toda a orientação, disponibilidade e partilha de conhecimento. Obrigado pela confiança depositada em mim.

A todos os membros e colaboradores do CICS, principalmente ao grupo "Biotechnology and Biomolecular Sciences", quero agradecer a grande entreajuda e bom ambiente proporcionado. Particularmente, à Margarida Grilo e à Fátima Santos agradeço a imprescindível ajuda que me deram ao longo do ano. À Carla Pereira, minha fiel parceira de laboratório, um enorme obrigado por estar sempre presente em todos os momentos e por me ajudar a ultrapassar todas as dificuldades que surgiram.

Finalmente, agradeço à minha família e amigos que sempre me acompanharam e apoiaram incondicionalmente, com um agradecimento especial ao João pelo constante e incansável apoio e carinho.

2. Resumo

A catechol-*O*-metiltransferase (COMT) é uma enzima que cataliza a transferência de um grupo metilo da S-adenosil-$_L$-Metionina para um grupo hidroxilo de uma grande variedade de substratos com estrutura catecólica, incluindo estrogénios e neurotransmissores como a dopamina e a noraepinefrina. A proteína é expressa na forma solúvel (SCOMT) e na forma membranar que contém 50 resíduos adicionais na extremidade N-terminal (MBCOMT). Numa elevada percentagem dos tecidos humanos, a COMT encontra-se presente sob a forma solúvel e apenas uma pequena fração como MBCOMT. O gene humano da COMT tem um polimorfismo comum num resíduo que resulta numa substituição de uma metionina por uma valina no resíduo 108 da proteína solúvel e no resíduo 158 da forma membranar. Os dois alelos têm sido associados a diversas doenças neurológicas, como esquizofrenia, anorexia nervosa e transtorno obsessivo-compulsivo. Assim, devido ao papel da COMT em várias desordens mentais, medições precisas e seletivas são requisitos essenciais para o melhoramento da investigação clínica da COMT. Deste modo, neste trabalho é desenvolvido uma metodologia seletiva e de baixo custo para quantificar a proteína COMT em lisados de *Pichia pastoris* por cromatografia líquida acolpada à espetrometria de massa (LC-MS/MS). O método foi validado de acordo com orientações internacionais, avaliando a seletividade, linearidade, precisão e exatidão, limite de deteção e limite de quantificação, *carry-over* e efeito de matriz. Todos os parâmetros avaliados encontraram-se dentro nos limites estabelecidos. O método foi capaz de quantificar as duas isoformas em amostras complexas como lisados celulares, demonstrando a sua aplicabilidade. A versatilidade do método analítico proposto poderá permitir a sua aplicação em análises de rotina laboratorial de SCOMT e MBCOMT em diversas matrizes biológicas como sangue, tecidos mamários, hepáticos ou cerebrais.

Palavras-chave

Pichia-Pastoris, catechol-*O*-metiltransferase solúvel, catechol-*O*-metiltransferase membranar, *Multiple Reaction Monitoring*, quantificação

3. Resumo alargado

A enzima catecol *O*-metiltransferase (COMT) cataliza a transferência de um grupo metilo da S-adenosil-$_L$-Metionina (SAM) para o grupo hidroxilo de um substrato catecólico, na presença de um catião divalente como o magnésio. Entre os inúmeros substratos fisiológicos da COMT encontram-se as catecolaminas neurotransmissoras (epinefrina, norepinefrina e dopamina), hormonas (como os estrogénios com estrutura catecólica), ácido ascórbico e catecóis xenobióticos.

Nos seres humanos, o papel fisiológico mais relevante da enzima é a eliminação de catecóis tóxicos ou biologicamente ativos. Para além disso, a COMT é um importante metabolizador de fármacos catecólicos (como $_L$-DOPA, metildopa e isoproterenol). Apenas existe um gene da COMT que codifica as suas duas isoformas, a solúvel (SCOMT) localizada no citosol e outra associada a membranas plasmáticas (MBCOMT), que contém 50 resíduos adicionais no N-terminal. A sua expressão é controlada por dois promotores distintos, P1 e P2. Apesar de a COMT existir em múltiplas formas polimórficas, existe um polimorfismo bastante comum em humanos que leva a mudanças da actividade enzimática. Esta alteração é causada pela transição de uma guanina para adenina (G -> A), no codão 108 da SCOMT e 158 da MBCOMT, resultando na substituição de uma valina para uma metionina. O gene da COMT tem sido fortemente associado a várias doenças psiquiátricas (esquizofrenia, anorexia nervosa, transtorno obsessivo-compulsivo) e mudanças na ativação cerebral. Devido a isto, o desenvolvimento de técnicas para uma rápida, económica e precisa quantificação das diferentes formas da COMT é crucial para a investigação clínica da enzima.

Primeiramente, neste trabalho, foi feita a produção das proteínas de interesse (SCOMT e MBCOMT) a partir de *Pichia Pastoris* X-33 Mut$^+$. De seguida, de modo a obter um padrão da enzima, a forma solúvel da COMT foi purificada através de cromatografia de afinidade por iões metálicos imobilizados (IMAC).

Posteriormente, neste trabalho foi desenvolvido e validado um método analítico de MRM capaz de detetar e quantificar a enzima COMT em amostras complexas, como lisados celulares de *Pichia pastoris*. O método foi validado de acordo com critérios internacionalmente aceites, da *Food and Drug Administration (FDA)* e da *International Conference on Harmonization (ICH)*. O método demonstrou ser seletivo para o analito e linear na gama de 25 a 200 µg mL^{-1}, com coeficientes de determinação (R^2) superiores a 0,99. Os limites de deteção e quantificação foram, respetivamente, de 3,3 e 25 µg mL^{-1} e a precisão e exactidão intra-dia apresentou-se abaixo dos 15%. O método não apresentou efeito de matriz nem *carry-over*.

A aplicabilidade do método foi avaliada por aplicação da metodologia a amostras digeridas de lisados de *Pichia pastoris* contendo SCOMT e MBCOMT. Globalmente, foi possível detetar e quantificar as duas isoformas nestas amostras complexas. Em conclusão, o método

desenvolvido é eficaz para a determinação da enzima COMT e poderá ser extrapolado em análises laboratoriais de rotina em matrizes como sangue, tecidos mamários, hepáticos e cerebrais .

4. Abstract

COMT is an enzyme that catalyses the transfer of the methyl group from S-adenosyl-L-methionine to the hydroxyl group of a large variety of catechols, including catechol-estrogens and the neurotransmitters dopamine and norepinephrine. The protein is expressed in both a soluble form (SCOMT) and a membrane-bound form with additional 50 residues at the N-terminal (MBCOMT). In most human tissues, the majority of COMT is present in soluble form and only a small fraction as MBCOMT. The human COMT gene has a common single-nucleotide polymorphism that results in substitution of methionine for valine at residue 108 of soluble protein and residue 158 of the membrane bound enzyme. The two alleles have been associated with several neurologic diseases, such as schizophrenia, anorexia nervosa and obsessive-compulsive disorder. Thus, due to the COMT's role in several mental disorders, accurate and selective measurements are essential requirements for improvement the COMT clinical investigation. Thus, in this work a specific and low-cost methodology is developed in order to measure COMT protein in *Pichia pastoris* lysates by liquid chromatography-multiple reaction monitoring (MRM) mass spectrometry. The method was validated according to international guidelines evaluating selectivity, linearity, precision and accuracy, limit of detection and limit of quantification, carry-over and matrix effects. All the evaluated parameters were found within the established confines. The method was able to quantify small amounts of both COMT isoforms in complex samples such as cell lysates, showing its applicability. The versatility of the analytical method proposed may allow its application in routine laboratory analysis of SCOMT and MBCOMT in various biological matrices such as blood, breast tissue, liver tissue or brain tissue.

Keywords

Pichia pastoris, Soluble catechol-*O*-methyltransferase, Membrane bound catechol-*O*-methyltransferase, Multiple Reaction Monitoring, quantification

5. Table of Contents

6. List of Figures

7. List of Tables

8. List of Acronyms

^{18}O	Oxygen-18
2DE	Two-dimensional gel electrophoresis
3-OMD	3-O-Methyldopa
A	Adenine
AADC	Aromatic amino acid decarboxylase
ACN	Acetonitrile
AQUA	Absolute quantitation
Asn	Asparagine
Asp	Aspartic acid
BA	Ammonium bicarbonate
BCA	Bicinchoninic acid assay
BMGY	Buffered Glycerol Complex Medium
BMMY	Buffered Methanol Complex Medium
BSA	Bovine serum albumin
CE	Collision energy
CID	Collision induced dissociation
COMT	Catechol-*O*-methyltransferase
CUR	Curtain gas
CV	Coefficient of variation
DIGE	Difference gel electrophoresis
DP	Declustering potential
DTT	Dithiothreitol
ELISA	Enzyme-Linked Immunosorbent Assay
ESI	Electrospray ionization
FDA	Food and Drug Administration
FIA	Flow Injection Analysis
FT	Fourier transformer
G	Guanine
GS1	Nebulizer gas
GS2	Heater gas
HCl	Hydrochloric acid
hMBCOMT	Human MBCOMT
HPLC	High performance liquid chromatography
hSOMT	Human SCOMT
ICAT	Isotope-coded affinity tag
ICH	International Conference on Harmonization
IMAC	Immobilized metal affinity chromatography
IS	Internal standard
IT	Ion trap
LC	Liquid chromatography
$_L$-DOPA	$_L$-3,4-dihydroxyphenylalanine
LLOQ	Lower limit of quantification
LOD	Limit of detection
LOQ	Limit of quantification
Lys	Lysine
m/z	Mass-to-charge ratio
MALDI	Matrix-assisted laser desorption/ionization
MBCOMT	Membrane bound catechol-*O*-methyltransferase
Met	Methionine
$MgCl_2$	Magnesium chloride
MRM	Multiple reaction monitoring
mRNA	Messenger RNA
MS	Mass spectrometry
OD_{600}	Cell density at 660 nm
PAI	Protein abundance index

PD	Parkinson's disease
PFC	Prefrontal cortex
Pro	Proline
PVDF	Polyvinylidene difluoride
Q	Quadrupole
Q1	First quadrupole
Q2	Second quadrupole
Q3	Third quadrupole
QC	Quality controls
R	Correlation coefficient
R^2	Coefficient of determination
RE	Relative error
RT	Retention time
SAH	S-adenosyl-$_L$-homocysteine
SAM	S-adenosyl-$_L$-methionine
SCOMT	Soluble catechol-*O*-methyltransferase
SDS	Sodium dodecyl sulphate
SDS-PAGE	Sodium dodecyl sulphate-polyacrylamide gel electrophoresis
SILAC	Stable isotope labeling by amino acids
SRM	Selected reaction monitoring
TIC	Total ion current
TOF	Time of flight
Tris	Tris(hydroxymethyl)aminomethane
Trp	Tryptophan
Val	Valine
WADA	World Anti-Doping Agency

Chapter 1 - Introduction

1.1. Catechol-*O*-methyltransferase (COMT)

Catechol-*O*-methyltransferase (COMT, EC 2.1.1.6) was described for the first time by Axelrod and co-workers in 1958 (1). Since then, COMT has been seen as an important enzyme in catecholamine biochemistry and pharmacology. More recently, this enzyme has shown a significant role in genetic mechanisms of variation in catechol metabolism and its clinical implications (2).

1.1.1. Physiological role of COMT

COMT is an enzyme that catalyzes the transfer of the methyl group of S-adenosyl-$_L$-methionine (SAM) to the hydroxyl group of the catechol substrate in the presence of a divalent cation such as Mg^{2+}. The result of this reaction is the *O*-methylated catechol and S-adenosyl-$_L$-homocysteine (SAH), a known COMT inhibitor, representing a negative feedback loop (3). After methylated, the substrate is inactivated and is no longer capable of performing its physiological function and becomes susceptible to additional conjugation reaction (4). The *O*-methylation occurs primarily at the 3-hydroxyl (*meta* position), but depending on the experimental conditions and the nature of the side chain of the catechol substrate, also varying the amount of the 4-methylated (*para* position), catechol are produced (5). Physiological substrates of COMT include catecholamine neurotransmitters (epinephrine, norepinephrine and dopamine), hormones (such as catecholestrogens), ascorbic acid, some indolic intermediates of melanin metabolism and xenobiotic catechols (4, 6, 7). COMT is regulated by steroids, estrogen and thyroid hormone analogs (8, 9). Besides, COMT expression is changed during normal brain development and in response to environmental (10) as well as its activity is different between genders (11). The major physiological role of COMT is the elimination of biological active or toxic catechols (12). COMT is also an important metabolizer of catechol drugs (e.g. $_L$-DOPA, methyldopa and isoproterenol) (4, 13) and has been suggested that plays a relevant role in modulating prefrontal cortex (PFC) dopamine neurotransmission (14-16). Besides, it protects the placenta and the developing embryo from activated hydroxylated compounds formed from aryl hydrocarbons by hydroxylases (17). The physiologically important role played by this enzyme has been widely demonstrated by several pharmacological studies indicating that *in vivo* inhibition of this enzyme by a variety of inhibitors or competitive substrates potentiates the physiological actions of catecholamines, which exert an innumerable of effects in a large variety of tissues (8).

1.1.2. COMT isoforms, structure and kinetics mechanisms

There are two COMT isoenzymes: a soluble form (SCOMT) and a membrane bound form (MBCOMT), with different roles in the metabolism of catecholamines and other catechol compounds (18). These isoforms share similar affinities for SAM (5) such as similar magnesium dependency, inhibition by calcium and a similar optimal pH for the activity (12). On the other hand, they differ from each other in their molecular weight, net surface charge (8), specificity and affinity for substrate (5), heat stability, response to a cation and enzymatic and kinetic properties (8). While SCOMT contain 221 amino acid residues and a molecular weight of 24.7 kDa, MBCOMT has an additional 50 amino acid residues in its amino terminal, a molecular weight of 30 kDa (19) and has a more negative charge (8). This extra peptide contains a stretch of 21 hydrophobic amino acid residues function as membrane anchor region (19) and contributes to the higher binding affinity of its substrates (5). MBCOMT has 10 to 100-fold higher affinity for catechol substrates than SCOMT (13) and a 10-fold higher binding affinity for the methyl donor SAM than the soluble form (6). However, SCOMT has much higher capacity (17). This means that at physiological low substrate concentration, MBCOMT would have much more preference for the *O*-methylation of catecholamines over SCOMT (5, 6). Both COMT isoforms favour 3-*O*-methylation (5).

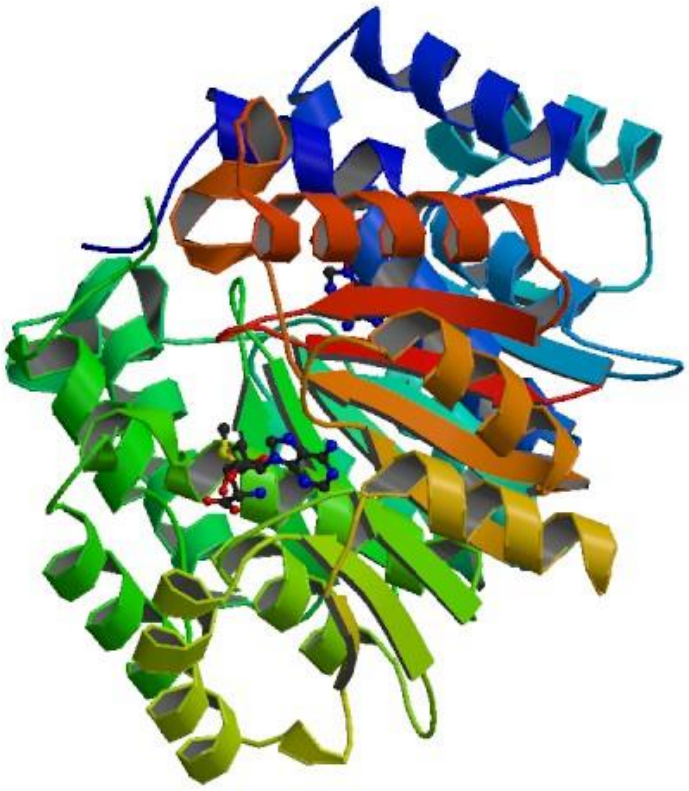

Figure 1 - The crystal structure of human catechol-*O*-methyltransferase complex with S-adenosyl-$_L$-methionine (20).

Vidgren and co-workers (1991) were the first to resolve the tree-dimensional structure of the rat SCOMT (21). Although there was no high-resolution structure of human COMT described, the human enzyme is probably similar to a rat structure because the amino acid sequence is 81% similar (14).

COMT has one-domain α/ß containing seven-stranded ß-sheet sandwiched between two sets of α-helices, five helices on one side and three on the other side. The strands are arranged in the order 3-2-1-4-5-7-6, where strand 7 is antiparallel to the others (Figure 1) (22, 23). This topology is characteristic of the SAM-dependent methyltransferase fold family (22). The active side of the enzyme is formed in the vicinity of the Mg^{2+} by residues from the amino terminal helices, through the SAM-binding fold (Rossman fold) to the loop in the C-terminal ß-strands (7, 21), which binds one magnesium ion and the catechol substrate, and the SAM-binding region. While SAM is buried within the structure of the enzyme, the catalytic site is a shallow groove located on the outer surface (12).

Methylation reaction follows a sequentially ordered mechanism (5). Firstly, SAM bound to COMT, followed by Mg^{2+}, which converts the hydroxyl groups of the catechol substrate to be more easily ionisable. The proton from that hydroxyl group is accepted by a COMT lysine residue (Lys144) which is close to those substrate groups. Then, the methyl group from SAM is transferred to the hydroxyl group. Lysine acts as a general catalytic base in this base-catalysed nucleophilic reaction. The Mg^{2+} has an octahedral coordination among two aspartic acid residues (Asp141 and Asp169), one asparagine residue (Asn170), one water molecule and among two catechol hydroxyls of the substrate (12, 17). Then, the "gatekeeper" residues (Trp38, Trp143 and Pro174) that form the hydrophobic "walls" join directly in the methylation reaction, by keeping the planar catechol ring in the correct position. These also define the selectivity of COMT toward different substrates (12, 17). Human COMT contains seven cysteines residues that probably exist as free thiol groups *in vivo*, but three of them are located in surface loops with their sulfur atoms exposed to solvent, making a potential site for intermolecular disulfide bond formation and protein aggregation (22).

1.1.3. COMT gene and polymorphisms

There is one single COMT gene, which encodes both SCOMT and MBCOMT. This gene is localized on the chromosome 22, band q11.2 and spans 28 kb (24) and contains six exons with the first two being noncoding. The expression of the COMT gene is controlled by two distinct promoters located in exon 3 (6). The distal 5' promoter (P2) regulates synthesis of 1.5 kb mRNA (Figure 2). This mRNA can code for both MBCOMT and SCOMT proteins by using the leaky scanning mechanism of translation initiation. The shorter transcript, 1.3 kb mRNA, is regulated by P1 promoter, which is located immediately before its start codon S-ATG and overlaps the start codon for MBCOMT. Furthermore, it can only code for SCOMT (6, 17). The regulation of the COMT gene expression seems to occur at transcription initiation, at translation initiation

and at mRNA splicing (7). Silencing gene through methylation may be a further regulatory mechanism (25).

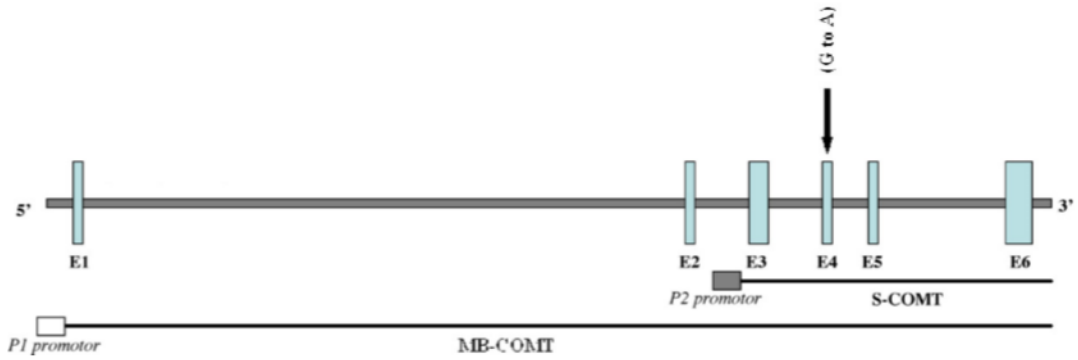

Figure 2 - Genomic structure of the COMT gene and the relative location of the Met/Val polymorphism (26).

COMT exist in a multiple polymorphic forms due to the present of occasional mutations in the gene (27). Withal, there is an extensively studied polymorphism of COMT gene that leads to changes in the enzymatic activity. This functional and common polymorphism is caused by transition from guanine to adenine (G -> A), at codon 108 of SCOMT or 158 of MBCOMT, resulting in a substitution of valine by methionine (Val108/158 -> Met108/158). Although the structures and catalytic activities of the two enzymes were similar, the Met108/158 form of COMT has a lower thermal stability and therefore a lower activity at physiological temperature (37 ºC), is more prone to inactivation through oxidation and has decreased protein levels *in vivo*. Thus, Val108/158 homozygotes have greater COMT activity and thermal stability and this genotype shows approximately one third more activity than Met108/158 homozygotes. Because the alleles are codominant, heterozygotes have intermediate levels of COMT activity (12, 13, 22, 25). The different activities of this COMT polymorphism result from the different thermal stability of the two enzymes forms and not from their kinetic properties, because that residue 108/158 does not contribute to the active site of COMT. It is located in the α5-β3 loop, completely buried within a hydrophobic pocket, about 15-20 Å from the binding side of SAM on the opposite side of COMT molecule (5, 22). COMT Val/Met due to differences in enzyme activity, alters dopamine levels in the prefrontal cortex. The Val108/158 homozygotes have an upregulation of dopamine D1 receptor densities which is a compensatory response for a lower dopamine tone, in cortical and limbic areas including prefrontal cortex. In contrast, Met108/158 homozygotes exhibit higher rates of prefrontal dopamine turnover, and thus higher dopamine availability and dopamine dependent signalling, which in turn contributes to differences in neural functioning (Figure 3) (28).

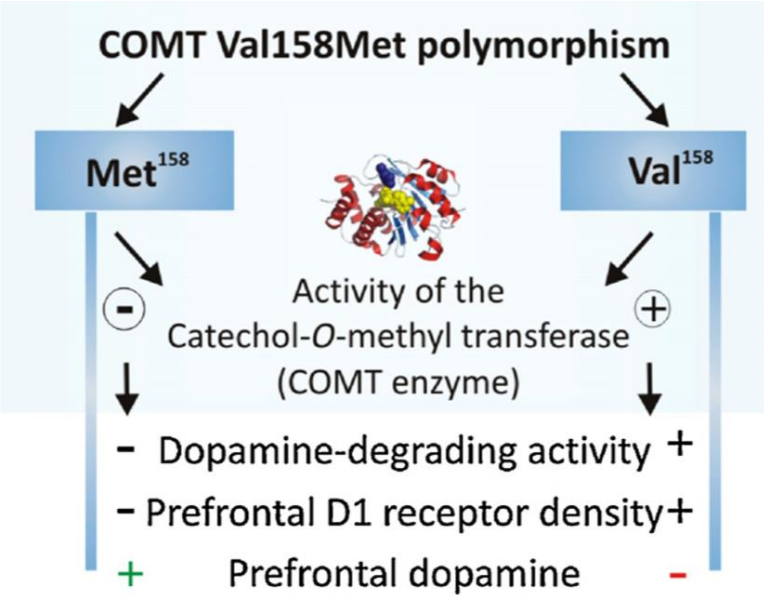

Figure 3 - Effects of the two alleles of COMT Val/Met in enzymatic activity and dopamine levels (adapted from (28)).

No equivalent polymorphism has been found in any other species and therefore, the Met108/158 may be specific to humans and it appears that COMT activity has decreased during evolution (2, 25). None of the other polymorphism reported for COMT appeared to have any physiological significance (27, 29).

1.1.4. Distribution of human COMT

COMT is present in prokaryotes and eukaryotes, namely bacteria, yeast, plants and animals, invertebrates and vertebrates (12). COMT is an intracellular enzyme and is widely distributed throughout the organs of the body, being found in practically all mammalian tissues investigated (17). However, the highest levels of COMT activity were found in liver, followed by kidney and the gastrointestinal tract, while the cardiac tissue has the lowest activity and skeletal muscle has none. In most tissues, COMT is larger present as SCOMT and only a small fraction as MBCOMT. Conversely, in the human brain (adrenal medulla), nearly 70% of the COMT activity is contributed by MBCOMT and only 30% by SCOMT (Figure 4), likely reflecting its higher affinity for the catecholamine neurotransmitters (6, 12, 18, 30, 31). In brain, COMT is located at the nerve ending region, central nervous system, cytoplasm of neurons, around the blood-brain barrier (ventricular ependymal cells, choroid plexus, leptomeninges, etc.) and in glial cells (13, 32). Besides that, COMT activity is mainly in the prefrontal cortex (16). In clinical studies, COMT activity is most conveniently determined in erythrocytes (18, 33). Also, changes in the level of COMT activity have been observed during mammalian development, along with ageing and in connection with the oestrus cycle (4).

About the subcellular localization, MBCOMT resides in intracellular membranes oriented on the cytoplasmic side of the rough endoplasmic reticulum, while SCOMT is mainly located in the cytoplasmic compartment and, also in the nuclei. The different distribution of S- and MBCOMTs in different subcellular compartments suggest that the contribution of each COMT to the methylation of a substrate in a given cell or tissue will not only depend on the kinetic properties of the enzymes of each substrate but also depend on the intracellular distribution characteristics of the enzymes as well as the substrate (6, 7, 34, 35).

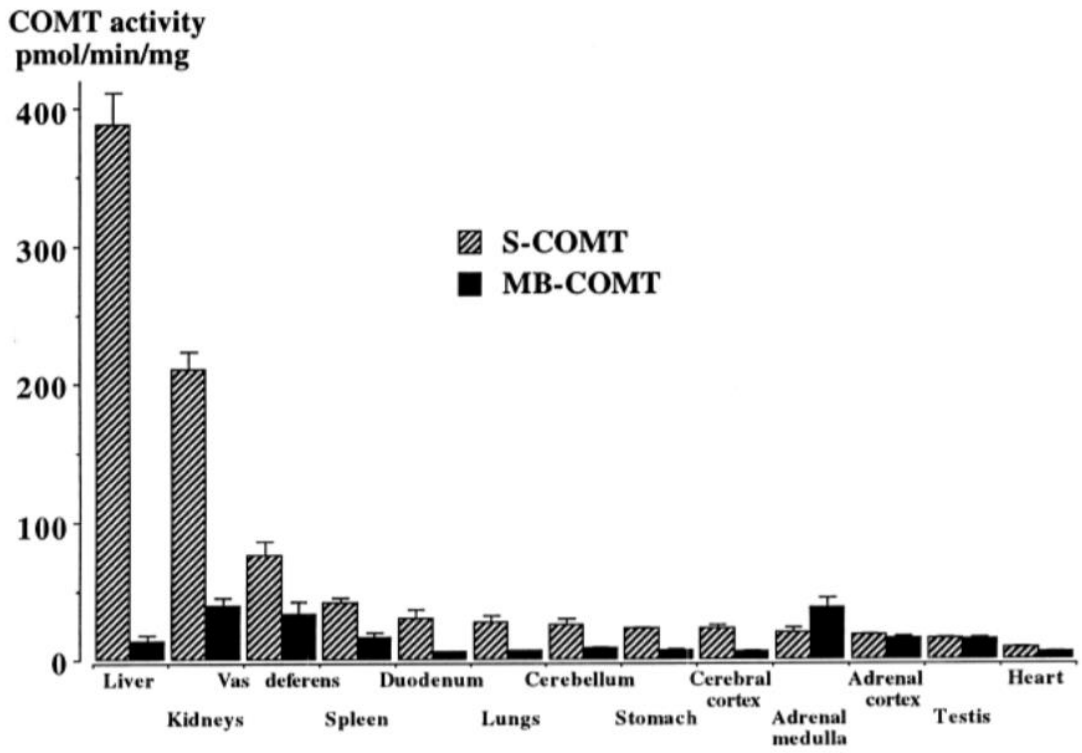

Figure 4 - Activities of SCOMT and MBCOMT in human tissues (adapted from (18)).

1.2. Relationship of COMT and human disorders

The catechol-*O*-methyltransferase gene has attracted strong neuroscientific interest due to its implication in dopaminergic neurotransmission. In particular, the literature has focused on the association between polymorphisms in the COMT gene and various cognitive phenotypes, psychiatric disorders and changes in brain activation and structure (26, 28). Despite many studies have failed, there are several works that have established significant correlations between the COMT genotype and human disorders (12). For example, studies in Chinese and Taiwan population (36) and Caucasian families (37) did not find a significant association with the developing schizophrenia. In contrast, two separate studies in European (38) and Asian population (39) indicated an effect of the Val158-allele for increasing the risk of

developing schizophrenia. In spite of many controversial results, the low allele (Met108/158) appears to have some association with aggressive and highly antisocial impulsive schizophrenia (40, 41), late-onset alcoholism (17), development of obsessive-compulsive disorder (9, 42), breast cancer (3, 4) and rapid cycling bipolar manic-depressive disorder (40). The high allele (Val108/158) was also associated with nervosa anorexia (43) and psychotic symptoms in Alzheimer's disease (44). Beyond that, higher proteins levels of soluble COMT in cancerous endometrium were found, in contrast with higher levels of membrane-bound COMT in controls endometrium (45). The importance of the COMT gene for the risk of psychiatric disorders like schizophrenia is strengthened by pathologies like the 22q11.2 deletion that includes the COMT gene and causes velocardiofacial syndrome, which has been associated with brain abnormalities including reduced overall brain volume, midline defects and regional grey matter reductions in parietal and frontal lobes, as well as impairments in executive functions and psychotic symptoms (9, 28, 42).

Succinctly, conflicting results might be due to the complex nature of the diseases under study, being constructs of different anatomical, physiological, endocrinological and psychological endophenotypes with regards to brain function (28).

1.2.1. Parkinson's disease

Parkinson's disease (PD) is the most common neurodegenerative movement disorders, affecting 1-2% of the population over the age of 60 years and above 6 million people worldwide (46). Consequences resulting from the unknown of certain mechanisms underlying the condition with the poor diagnostic accuracy, absence of valid biomarkers and difficulties to elaborate therapeutic interventions that might significantly influence disease progression (47). PD has been essentially regarded as a disorder of motor function, producing a variable, asymmetric and progressive combination of resting tremor, bradykinesia, rigidity and postural instability (47). The core motor feature of Parkinson's disease result from cell loss in the substantia nigra pars compacta and the degeneration of the nigrostriatal dopaminergic pathway (32, 48).

The main clinical interest in COMT relies on the possibility of using COMT inhibitors as adjuncts in the therapy of PD with $_{L}$-3,4-dihydroxyphenylalanine ($_{L}$-DOPA), precursor of dopamine (23, 32). Unlike dopamine, $_{L}$-DOPA crosses the blood-brain barrier and is then decarboxylated to dopamine by aromatic amino acid decarboxylase (AADC) and released by presynaptic terminal in the striatum replenishing the dopaminergic deficiency. Inhibition of COMT stops conversion of $_{L}$-DOPA to its metabolite 3-*O*-Methyldopa (3-OMD) which helps to increase the $_{L}$-DOPA extracellular level. Thus, $_{L}$-DOPA can be available for transport into the brain which causes symptomatic dopamine relief (Figure 5) (12, 32). Nowadays, the dopamine replacement therapy with $_{L}$-DOPA together with an inhibitor of aromatic amino acid decarboxylase and a COMT inhibitor is the most effective treatment in PD. Therefore, it

becomes clear the importance of developing more effective drugs for an effective COMT inhibition (19, 48).

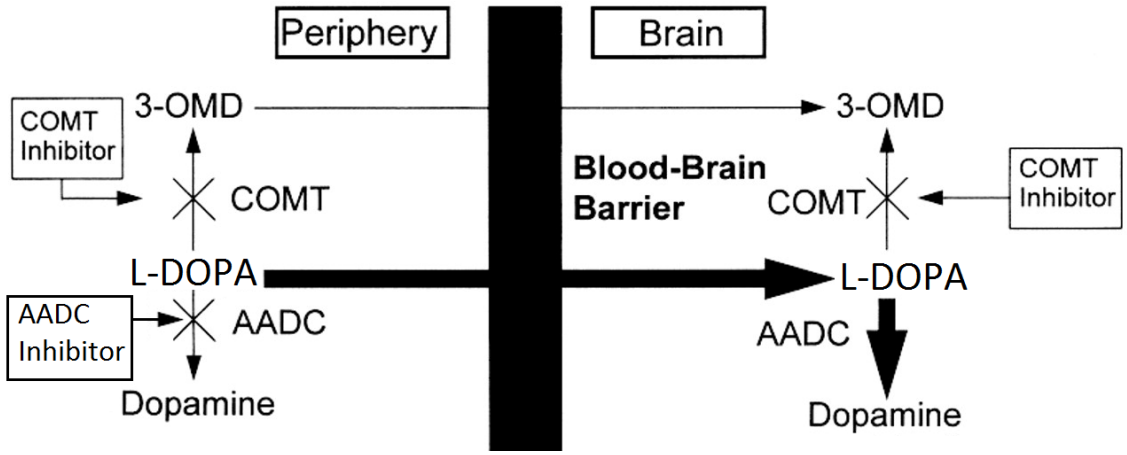

Figure 5 - Metabolisms of levodopa in blood-brain barrier (adapted from (21)).

1.3. Recombinant hSCOMT biosynthesis and purification

Recombinant technology is the best strategy to obtain large amounts of human proteins. Over the years, recombinant human SCOMT (hSCOMT) has been produced via different expression systems, such as transfected mammalian cells (35, 49), insect cells (baculovirus) (50), prokaryotic cells (*E. coli*) (6, 51, 52) and yeast (*P. pastoris*) (53). Each one has advantages and drawbacks (Table 1) to be taken into consideration in the selection of optimal expression system. The capacity of producing proteins at high levels, either intracellular or extracellular, and produce complex biomolecules that need to undergo posttranslational modification such as glycosylation, disulfide bridges formation and proteolytic processing, makes *Pichia pastoris* an ideal expression system for hSCOMT (54, 55).

Table 1 - Advantages and disadvantages of *E. coli*; yeast; insect cells and mammalian cells in the biosynthesis of recombinant human proteins (56).

	Advantages	Disadvantages
E. coli	✓ Rapid expression ✓ Less expensive ✓ Simple process scale-up ✓ Well characterized genetics	✖ No eukaryotic post-translational modification ✖ Some proteins are not properly folded ✖ Proteins are rarely secreted
Yeast (*P. Pastoris*)	✓ Moderately rapid expression ✓ Works well for secreted and intracellular proteins ✓ Well established large scale production and downstream processing	✖ Gene expression less easily controlled ✖ Enhanced safety precautions are required

	✓ Less expensive ✓ Most proteins folding and post-translational modifications are possible	
Insect cells (baculovirus)	✓ Moderately rapid expression ✓ Works well for secreted, membrane and intracellular proteins ✓ Most protein folding and post-translational modification are possible	✖ Expensive ✖ Difficult to scale-up ✖ Lack of information on glycosylation mechanism
Mammalian cells	✓ Works well for secreted and membrane proteins ✓ All proteins folding and most authentic post-translational modifications are possible	✖ Expensive ✖ Yields of intracellular proteins are low ✖ Difficult to scale-up

Typically, a high degree of COMT purity is a prerequisite for several laboratory applications, namely, kinetics trials, structural resolution and docking simulation. During the last decades, several purification procedures were been described to COMT. Usually, COMT protein has been isolated by chromatography procedures, such as size exclusion (57), anion (57-59) or cation exchange chromatography (60, 61), reversed-phase (57), hydrophobic interaction chromatography (51, 62) and by affinity chromatographic methods (14, 63). More recently, Immobilized Metal Affinity Chromatography (IMAC) was described by Pedro and co-workers (53) as an extremely efficient and selective strategy for the direct capture of hexahistidine tagged SCOMT with a great degree of purity and a high percentage of protein recover from recombinant *P. pastoris* lysates. Therefore, this methodology was selected as purification strategy of target proteins.

1.4. Methods for protein quantification

Precise and exact quantification of proteins is essential for understanding, detecting and controlling many diseases. In the specific case of COMT, due its role in several mental disorders, accurate and selective measurements are essential requirements for COMT clinical investigation.

The difficulty in purifying proteins makes its quantification an analytical challenge (64). Spectrophotometric methods such as ultraviolet absorption, Bradford, Lowry and bicinchoninic acid (BCA) assays are usual used to quantify total protein content of a solution. The ultraviolet absorption methods estimates the amount of protein by measuring the characteristic absorption of tyrosine and tryptophan at 280 nm or peptide bond at 205 nm (65). The principle of Bradford assay involves the binding of Coomassie Brilliant Blue G-250 to protein at acid pH that causes a

shift in the absorption maximum of the dye from 465 to 595 nm (66). Both Lowry and BCA assays depends on the reduction of Cu^{2+} to Cu^{+} by proteins in alkaline solutions (Biuret reaction). While BCA is one step assay and results of an intense purple colour with an absorbance maximum at 562 nm (67), Lowry assay requires one more step after Biuret reaction, which is the reduction of the Folin-Ciocalteu reagent producing a characteristic blue colour with absorbance maxima at 750 nm (68). These spectrophotometric methods are sensitive, simple, inexpensive and fast, but they are not protein specific and require an appropriate protein standard or constituent amino acid sequence information to make an estimate of concentration value (64, 65).

On the other hand, proteins and peptides in biological matrices have been quantified by enzyme-linked immunosorbent assay (ELISA) and Western blot, which works by applying antibodies, with high specificity and sensitivity. However, these methods are limited by the considerable time and cost invested in the development of antibody reagents for each target protein. Also, they have an insufficient selectivity and not enabling distinction between the peptide and its derivatives or degradation fragments (69, 70).

Beyond immunological methods one can also achieve protein quantification using gel-based approaches (DIGE) where quantification is achieved following 2DE and relies on pre-electrophoretic labelling of samples with one of three spectrally resolvable fluorescent CyDyes (Cy2, 3 and 5), allowing multiplexing of samples into the same gel (71). Although the method can provide the ability to detect many post-translational modifications and detecting hundreds to thousands of spots in one single gel, these assays have some limitations: they are expensive since many gels are required to achieve statistically valid results. Furthermore, it takes a long time for gel perform and analysis and it is difficult to determine low abundance proteins which makes unfeasible to look for smaller changes (71, 72).

Thereby, mass-spectrometry-based quantification methods have gained increasing popularity over the last years. The advantages of these methods are precision, sensitivity, throughput and convenient automation (73).

1.5. Mass spectrometry for protein analysis

Mass spectrometry (MS) is commonly used for identification and quantification of a wide range of analytes such as drugs, lipids, proteins and peptides (74). It is an analytical technique that measures the mass-to-charge ratio (m/z) of ions based upon their motion in an electric or magnetic field. The instrumentation consists of three parts: an ionization source, a mass analyzer and a detector (Figure 6). Sample molecules are converted into ions in the gas phase by an ionization source formed positively or negatively charged ions which then are separated according to their m/z ratio using a mass analyser and finally detected (75). Proteins or peptides can be ionized by electrospray ionization (ESI) or matrix-assisted laser desorption/ionization (MALDI). The difference between both is that the MALDI sublimates and ionizes the samples out of a dry, crystalline matrix via laser pulses, while ESI ionizes the samples

out of a solution and are usually coupled to liquid-based separation tools. MALDI-MS is normally used to analyse relatively simple peptide mixtures, whereas integrated liquid-chromatography ESI-MS systems (LC-MS) are preferred for the analysis of complex samples. Usual mass analyzers for detection and analysis of biomolecules are the time of light (TOF), quadrupole (Q), ion trap (IT), Fourier transformer (FT) and orbitrap mass analyzers (73).

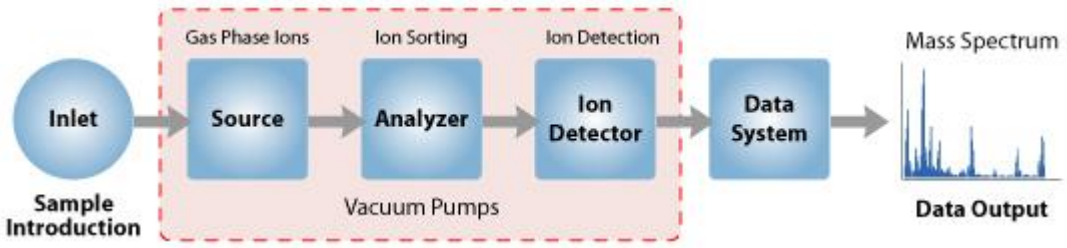

Figure 6 - Components of a Mass Spectrometer (52).

The traditional way for analysis of proteins is managed on the peptide level (bottom-up). Proteins are digested by a protease such as trypsin (cleavage after lysine or arginine) and the resulting peptides can be analyzed directly in a mass spectrometer or after separation common via liquid chromatography (69, 74). Although not usual, is also possible to obtain sequence information directly from full-length proteins (top-down) (76). The intact protein mass is first obtained by the mass spectrometer and isolated for MS/MS analysis by dissociation techniques (e.g. CID) to provide sequence information (69). Compared to full-length proteins, peptides are more easily ionized in the mass spectrometer leading to an increased sensitivity [57].

Protein quantification can be done by peptide labelling or using label-free methods (Figure 7). The first approach uses stable isotopes to label peptides, introducing a mass difference between the labelled and unlabelled peptides that can be recognized by a mass spectrometer leading to a relative quantification (77). These mass tags can be introduced into proteins or peptides metabolically (SILAC), by chemical means (ICAT, iTRAP), enzymatically (^{18}O), or provided by spiked synthetic peptide standards (AQUA)(78). On the other hand, label-free quantification (PAI, TIC) aims to provide quantitative information without introducing any form of labelling. These methods present many advantages over labelled strategies: they are fast, cost-effective and uncomplicated since no additional sample preparation is required (72, 77).

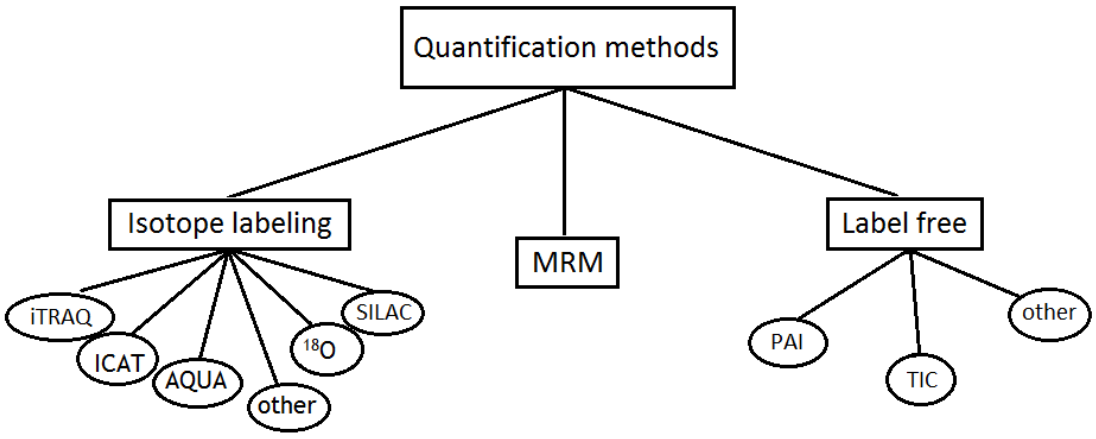

Figure 7 - Typical quantification strategies (Adapted from (77)).

1.5.1.1. Multiple reaction monitoring mass spectrometry

In addition, Multiple Reaction Monitoring (MRM) or Selected Reaction Monitoring (SRM) is a targeted MS/MS method that has been used in analysis of small molecules before being used in proteomics. It has emerged as a very promising technique for protein and peptide quantification in alternative to immunoassays (70, 77). Quantitative study of a specific set of, *à priori*, known proteins is the aim of MRM. Selected peptides for these proteins are featured by monitoring transitions, which are the precursor-fragment ion pairs isolated by MS (77). Thus, this method requires only knowledge of the masses of the selected peptide and its fragments ions (70).

Relating to logistics, triple quadrupole mass spectrometers are typically used for MRM experiments, which have three serially placed quadrupole mass analyzers (Figure 8). The first (Q1) and the third quadrupole (Q3) are used to scan for ions, while the second quadrupole (Q2) is worn as a collision cell and to transmit all fragment ions to Q3. Only the specific m/z ratio(s) of the pre-selected precursor ion(s) is transmitted through the Q1, whilst all others ions are ignored. The precursor ion(s) is fragmented by collision-induced dissociation (CID) in Q2, and thereafter all resulting fragment ions (daughter ions) are transmitted to the Q3. In third quadrupole, only ions corresponding to the pre-set m/z rations of selected fragment ion(s) are transmitted to the detector, while all ions will be excluded (74).

The great advantages of these techniques are the ability to quantitative a large number of analytes in a single scalable measurement process, low limit of quantification, cost-effective, high throughput and analytical reproducibility (70). These overcomes ensure high

accuracy, sensitivity and specific detection of analytes in complex matrices, including wholes blood, plasma and cell lysates, since a signal is registered only when a pre-selected fragment ion is produced by a pre-selected precursor (70, 74, 79, 80).

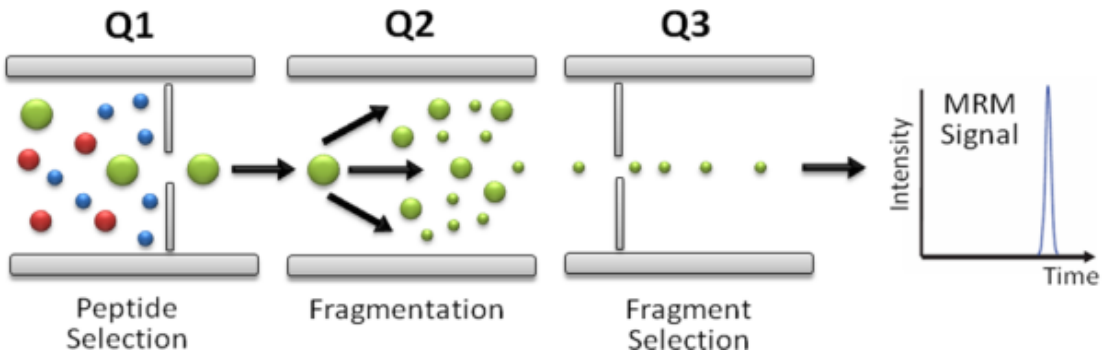

Figure 8 - Functional outline of a MRM equipment (81).

1.5.1.1.1. Target peptide selection

During the design of MRMs trials, it is recommended to use specific peptides from each protein. The selection of proteotypic or signature peptides is the first and most critical step in MRM analysis of target proteins (70, 74).

These peptides must have several intrinsic characteristics. Foremost, selected peptides must be unique to the protein(s) which will be monitored and be distinguishable from matrix ions. They should ionize and fragment well, providing abundant ions in the mass spectrum and more sensitive assay. Also they must ensure that the mass to charges ration (m/z) of the selected peptides is compatible with the mass range of the instrument used (70, 74). Beyond that, peptides that contain amino acids that are prone to post-translational modifications and with potential artefactual modifications during samples preparation should be avoided. Whereby peptides containing cysteine and methionine should not be used, since cysteine is typically modified during sample preparation and due to methionine ability to undergo oxidization. Moreover, peptides containing histidine should be discarded because the possibility of alterations in the side chain charge. Because asparagine and glutamate are prone to deamination and N-terminal glutamine or glutamate form pyroglutamate, peptides containing these characteristics should also not be included. Furthermore, peptides with missed cleavages or non-tryptic cleavage sites should also not be used (70, 74, 82).

Finally, when it is not possible to avoid these peptides, it will be crucial to monitor both the modified and the unmodified versions of the peptide (70, 74).

1.5.1.1.2. MRM transition selection and optimization

After the selection of peptides, the most sensitive and robust transitions of target peptides must be chosen. Due to formation of multiple charged ions when peptides are protonated during ESI, the *m/z* rations have a large variation. Beyond that, multiple peaks can be observed from each peptide, since different degrees of protonation will coexist. Therefore, it is crucial the selection of transitions specific for the fragment which reveal the better signal (70). In general, fragmentation results in the production of two complementary peptide ion series: y-ions and b-ions. While y-ions retains a positive charge at its C-terminal end, b-ions retains the charge at the N-terminal end (70). The y-ions are typically the better choices because are more stable during fragmentation (74).

Usually, the best two to four transitions per peptide are chosen and for each precursor peptide (precursor ion) two or more peptide fragments (fragment ions) are selected for quantitative assays (70, 74).

Due to differences in fragmentation patterns between mass spectrometers, it is important to optimize each peptide individually to set the best balance of signal to noise. The parameters that can be optimized to improve instrument performance and sensitivity in an MRM assay include source-dependent and scan-based parameters (74). The first holds parameters such an IonSpray voltage, temperature and gas settings (CUR, GS1 and GS2). The IonSpray parameter controls the voltage applied to the sprayer, which ionizes the sample in the ion source. It depends on the polarity, and affects the stability of the spray and the sensitivity (74, 83). With regard to gas settings, curtain gas (CUR) prevents ambient air and solvent droplets from entering and contaminating the ion optics, while allowing the input of sample ions. Nebulizer gas (GS1) helps generate small droplets of sample flow, while the heater gas (GS 2) aids in the evaporation of solvent, which helps to increase the ionization of the sample. The optimal temperature is the lowest temperature at which the sample is vaporized completely. These parameters tend to be constant from day-to-day, but can vary gradually over time (70, 74). Scan-based parameters are specific to each of the transitions included in the method that include, besides the ion transitions, the transmission windows for Q1 and Q3, the collision energy (CE) and the dwell time for each transition. The transmission window sets the mass range that is transmitted through Q1 and Q3 for a transition. The CE parameter controls the potential difference between Q0 and Q2 (collision cell), and it is the amount of energy that the precursor ions receive and fragment. Finally, dwell is the time in milliseconds that the system takes to scan a particular transmission (70, 74).

Sophisticated bioinformatics tools have been developed for MRM method optimization and data analysis including MRMpilot, Pinpoint, and Skyline (84). More specifically, Skyline is an open-source platform for data interpretation that provides and generates critical information for experimental design and analysis of MRM. Peptide transition lists are generated

by refinement of proteomic peptide lists from protein sequences or database entries, both by utilizing online MS/MS spectral repositories and by supporting the generation of custom-built libraries. It has an advantage over the other options being freely available for academic and commercial use (84, 85).

Chapter 2 – Aims

Owing to role of the COMT into several disorders, a fast, low-cost and precise measurement of this protein in complex samples are essential for COMT clinical investigation. Thus, this work is divided into three main objectives, which are:

- ✓ Produce recombinant SCOMT_6His and MBCOMT_6His and purify the soluble form.
- ✓ Develop and validate a high specific methodology for detection and assessment of SCOMT by liquid chromatography-multiple reaction monitoring (MRM) mass spectrometry.
- ✓ Evaluate the applicability of the propose methodology in *Pichia pastoris* lysates containing one or both COMT isoforms.

Chapter 3 – Materials and Methods

3.1. Materials

Ultrapure reagent-grade water was obtained with a Mili-Q system (Milipore/Waters). Acetonitrile and water (MS-grade) from Fisher were acquired from Enzymatic (Santo Antão do Tojal, Portugal). Zeocin were obtained from Invitrogen (Carlsbad, CA). Yeast nitrogen base (YNB), glucose, agar, yeast extract, peptone, dithiothreitol (DTT), glycerol, glass beads (500 µm), ureia, tripsin and formic acid (for mass spectrometer) were purchased from Sigma Chemical Co. (St. Louis, MO). The NZYcolour Protein Marker II used for estimation of subunit molecular weight was purchased fromNZYTech (Lisboa, Portugal). Bis-Acrylamide 30% was obtained from Bio-RAD (Hercules, CA). The High-Range Rainbow molecular weight markers used for estimation of subunit molecular weight and iodoacetamide and anti-rabbit IgG alkaline phosphate secondary antibody were purchased from GE Healthcare Biosciences (Uppsala, Sweden) while monoclonal rabbit COMT antibody was purchased from Abcam (Cambridge, England). The Glu1-Fibrinopeptide B was purchased from AB Sciex (Framingham, USA). All chemicals used were of analytical grade, commercially available, and used without further purification.

3.2. Methods

3.2.1. Plasmid and bacterial strain

The plasmid pICZαA-hSCOMT_His6 (Invitrogen Corporation, Carlsbad, CA, USA) was used for recombinant SCOMT production on *Pichia pastoris* X-33 Mut^+ strain. For recombinant MBCOMT production, it was used the plasmid pICZαA-hMBCOMT_His6 (Invitrogen Corporation, Carlsbad, CA, USA) on *Pichia pastoris* X-33 Mut^+ strain.

3.2.2. Recombinant human SCOMT and MBCOMT production and recuperation

P. pastoris cells were grown for 72 hours at 30 ºC in YPD medium plates (1% yeast extract, 2% peptone, 2% glucose and 2% agar) containing 200 µg mL^{-1} Zeocin. A single colony was inoculated in 100 mL of BMGY (100 $mmol^{-1}$ potassium phosphate buffer (pH 6.0), 1.34% yeast nitrogen base, 4×10^{-4} g L^{-1} biotin and 1% glycerol) in 500 mL shake-flasks and grown overnight at 30 ºC and 250 rpm to a cell density at 600 nm (OD_{600}) typically 6. Then, an aliquot of the fermentation in the medium BMGH was collected and centrifuged (500 xg, 5 min) to remove glycerol and was added to 125 mL of BMMY medium (100 mmol L^{-1} potassium phosphate buffer (pH 6.0), 1.34% yeast nitrogen base, 4×10^{-4} g L^{-1} biotin and 0.5% methanol) in 500 mL

shake-flasks to an initial OD_{600} fixed to 1.0 unit. After a 24 hours growth at 30 ºC and 250 rpm, cells were harvested by centrifugation (1500 xg, 10 min, 4 ºC) (53).

Thereafter, cells were lysed in equilibrium buffer (150 mmol L^{-1} NaCl, 10 mmol L^{-1} DTT, 50 mmol L^{-1} Tris, 1 mmol L^{-1} $MgCl_2$, pH 8.0) at a ratio of 1:2:2 (1 g cells, 2 mL lysis buffer and 2 g glass beads). Lysis was accomplished through the application of a sequential procedure with glass beads of 7 cycles of vortexing for 1 min with 1 min of interval on ice. Subsequently, the mixture was centrifuged (500 g, 5 min, 4 ºC) and the pellet obtained was resuspended in the chromatographic binding buffer (500 mmol L^{-1} NaCl, 50 mmol L^{-1}, Tris 1 mmol L^{-1} $MgCl_2$ and 5 mmol L^{-1} Imidazol at pH 7.8) (53).

3.2.3. Immobilized metal affinity chromatography for SCOMT purification

Chromatographic experiments were performed in an ÄKTA Avant system with UNICORN 6.1 software (GE Healthcare, Uppsala, Sweden). The chromatographic experiments were performed on HisTrapTM FF crude (5 mL), a prepacked IMAC stationary phase with nickel ions (GE Healthcare, Uppsala, Sweden). All buffers pumped into the system were prepared with Mili-Q system water, filtered through a 0.2 µm pore size membrane (Schleicher Schuell, Dassell, Germany) and degassed ultrasonically. The column was initially equilibrated with 500 mmol L^{-1} NaCl, 50 mmol L^{-1} Tris, 1 mmol L^{-1} $MgCl_2$ and 5 mmol L^{-1} Imidazol at pH 7.8. Aliquots of resuspended pellet in equilibration buffer at a ratio of 1:5 (1 g cells to 5 mL buffer), were injected onto the column using a 2 mL loop at a flow rate of 0.5 mL min^{-1}. After elution of the unretained species, the flow rate rise to 1 mL min^{-1} and imidazole concentration was increased from 0 to 50 mmol L^{-1} at for 5 column volumes (CVs), followed by a step at 70 mmol L^{-1} of imidazole (5 CVs), other at 300 mmol L^{-1} of imidazole (5 CVs) and finally at 500 mmol L^{-1} (5 CVs) (53).

In all chromatographic runs, the conductivity, pH, pressure and absorbance at 280 nm were continuously monitored. The target hSCOMT fractions were collected at 300 mmol L^{-1} of imidazole, pooled according to the chromatograms profile obtained and concentrated and desalted with Vivaspin concentrators (10.000 MWCO).

3.2.4. SDS-PAGE and Western Blot

Reducing Sodium Dodecyl Sulphate-Polyacrylamide Gel Electrophoresis (SDS-PAGE) and western blot were performed according to the method of Laemmli (86) and as previously described (87). Samples were prepared in loading buffer (500 mmol L^{-1} Tris-CL (pH 6.8), 10% (w/v) SDS, 0.02% bromophenol blue (w/v), 0.2% glycerol (v/v), 0.02% 2-mercaptoethanol (v/v)) at ratio of 3:1 (30 µL sample to 10 µL loading buffer) and were denatured at 100 ºC for 5 min. The run was performed on 4% stacking gel and 15% resolving gel containing 0,1% SDS with a

running buffer (25 mmol L^{-1} Tris, 192 mmol L^{-1} glycine, 0.1% SDS (w/v)) at 120 V for 1 h 40 min. Then, gel was stained by blue Coomassie (87).

For Western Blot, the gel was transferred to a polyvinylidene difluoride (PVDF) membrane. In this case, proteins were transferred over a 40 min period at 750 mA at 4 ºC in a buffer containing 10 mmol L^{-1} CAPS and 10% (v/v) of methanol. After the blotting, the membranes were blocked with TBS-T (pH 7.4) containing 5% (w/v) non-fat milk for 60 min at room temperature, washed 3 times during 15 min and exposed overnight at 4 ºC to a rabbit anti-rat SCOMT polyclonal antibody, that cross reacts with the human protein, at 1:1000 dilution in TBS-T 1%. The filters were washed three times during 15 min with TBS-T and adherent antibody was detected by incubation for 1 h with an anti-rabbit IgG alkaline phosphatase secondary antibody at 1:40000 dilution in TBS-T 1%. The PVDF membranes were air dried, incubating with 1 ml of ECL for 5 min and enhanced by exposure to chemiluminescence's detection (87).

3.2.5. In-gel digestion

In-gel digestion was performed only for the development of SCOMT standard. This protocol was implemented and adjusted from Shevchenko and co-workers (88).

After cut the SCOMT protein band, the gels pieces were washed three times in wash solution (50% acetonitrile (ACN), 25 mmol L^{-1} ammonium bicarbonate (BA)) at 37 ºC in constant agitation during 15 min each. Then, acetonitrile was added to the gels and incubate at room temperature until gel pieces become white and shrink. All acetonitrile was removed by speed vacuum. After that, the gel pieces suffer reduction by adding 10 mmol L^{-1} DTT in 25 mmol L^{-1} BA and incubated 60 min at 56 ºC. Then, the liquid is removed and the gels were alkylated by adding 55 mmol L^{-1} IAA in 25 mmol L^{-1} BA and incubated in dark at room temperature during 30 min. The gel pieces were washed again three times in wash solution and saturated with trypsin (20 ng μL^{-1}), 40% BA and 9% ACN during 60 min in ice. Subsequently, the gel pieces were incubated overnight at 37 ºC for protein digestion. Thereafter, the liquid was removed to new tubes and the peptides were extracted by adding 0.1% AF, 0.1% AF in 50% ACN and 0.1% AF in 80% ACN. Between each addition, gel pieces were incubated for 15 min at 37 ºC and the resultant liquid was removed to the new tubes. Finally, the resultant liquid of the new tubes was dry by speed vacuum and stored at -20 ºC until used (88).

3.2.6. Total protein quantification

Protein content in complex samples (cell lysates) was measured by the Pierce BCA Protein Assay Kit (Thermo Scientific, USA), using BSA as the standards (0.025 – 2.0 mg ml^{-1}), according to manufacturer's instructions.

3.2.7. In-solution digestion

In-solution digestion was performed for the digestion of complex samples, such as cell lysates, containing SCOMT and MBCOMT. This protocol was adjusted from Medzihradszky (89).

The sample was dissolved in a buffer with 50 mmol L^{-1} Tris-HCl (pH 8), 5 mmol L^{-1} DTT and 8 mmol L^{-1} Urea to a final concentration of approximately 1 mg mL^{-1} and incubated 60 min at 37 ºC. After cooling to room temperature, iodoacetamide was added to a final concentration of 50 mmol L^{-1} and the sample was incubated 40 min at room temperature. To reduce the urea concentration, the sample was diluted 10 times in buffer 50 mmol L^{-1} BA. Then, the sample was digested by adding a trypsin solution (20 ng μL^{-1}) with 40% BA and 9% ACN in ratio 1:10 (v/v) to a final ratio of 1:20 between tripsin:protein in sample; and incubated for 16 hours at 37 ºC. To stop the digestion, formic acid was added to a final concentration of 5% (v/v).

3.2.8. Total peptide quantification

Peptide content in samples was measured by the Pierce™ Quantitative Colorimetric Peptide Assay Kit (Thermo Scientific, USA), using Peptide Digest Assay Standard as the standards (0.0156 – 1.0 mg ml^{-1}), according to manufacturer's instructions.

.

3.2.9. Peptide sample preparation

The samples were concentrated and desalted by using reversed-phase C18 Zip-Tips ™ (Millipore, Bed- ford, MA, USA) according to the manufacturer's recommendations. Peptides were eluted in 10 µL of 80% ACN with 0,1% formic acid and made up with water with 0.1% formic acid until achieved a final volume of 40 µL. Then, every samples were spiked with 5 µL of Glu1-fibrinopeptide B 1350 fmol μL^{-1} (Intern Standard - IS).

3.2.10. Determination of the ideal MRM transition using skyline program

It was used an in silico method utilizing the Skyline program to determine the optimal MRM transition precursor (Q1) and fragment (Q2) ions. The FASTA file for COMT was acquired from a well-known freely accessible database of protein sequences, called UniProt (90). Then, this file was imported into the Skyline program (91) and its precursor and fragment ions were generated by performing *in silico* trypsin digestion. The peptides were used according to the rules described above and the precursor length range was set at 8 to 25 amino acids. Beyond

that, it was used an online tool SRM Collider for compare transitions to all others in a given background proteome and find interferences. This approach is currently applied for identify characteristic transitions. The Skyline transitions were imported into SRM Collider (92) and the conditions were pre-selected with the exception of the genome which was selected as Human PeptideAtlas (tryptic).

3.2.11. Liquid chromatography tandem-mass spectrometry (LC-MS/MS) operation conditions

This protocol was adjusted from Chen and co-workers (93) and Kay and co-workers (94).

Absolute quantification was performed using a JASCO X-LC™ system (3167CO, 3080DG, 3159AS, 3185PU) connected with a 4000 QTrap (AB Sciex) equipped with a Turbo V™ Ion Source operating in the positive ion mode. The software used for controlling this equipment and analyzing the data was Analyst Version 1.6.1 (AB Sciex). Samples were detected in a multiple reaction monitor (MRM) mode. For the optimization of MRM parameters of Glu1-Fibrinopeptide B, the peptide was infused with mobile phase at a flow-rate of 10 µL min^{-1} using a syringe pump (Harvard Apparatus, Holliston, MA, USA). The optimization of MRM parameters of COMT was done through the Flow Injection Analysis (FIA) compound optimization. For each run was injected a total of 5 µL of sample and the peptide separation was achieved in 20 min on Synergi 4U Fusion-RP 80A column (50 × 2.0 mm, 4 µm, Phenomenex) at a flow rate of 100 µL min^{-1}. The mobile phases were (A) 0.1% formic acid in water and (B) 0.1% formic acid in acetonitrile. After an isocratic step of 2 min at 2% phase B, a linear gradient from 2% to 30% B was run over the next 8 min, then was an isocratic set of 4 min at 80% phase B followed by a linear gradient from 80% to 2% B and finally a 4 min of an isocratic gradient at 2%. All source (temperature, IonSpay, GS1, GS2 and CUR) and compound parameters (DP, CE) were subjected to optimization. The 4000 QTrap optimal instrument source parameters were ion spray voltage at 5000 V, the heater gas temperature at 550 ºC, a nebulizer gas (GS1) of 80 Pa, a heater gas (GS2) of 50 Pa and a curtain gas of 20 Pa. Optimal conditions of final MRM transitions, declustering potential (DP), collision energy (CE), Dwell are shown in Table 2. Peak areas were integrated using the MultiquantTM 2.1.1 software (ABSciex).

Table 2 - Conditions of MRM transitions evaluated in this work.

	Q1	Q3	Dwell	ID	Charge	DP	CE
COMT	632.966	845.430 279.097	20	YDVDTLDMVFLDHWK	+3	77.3	26.7
	840.998	1169.652 485.308 413.275		VTLVVGASQDIIPQLK	+2	120.0	50.0
Glu1-Fibrinopeptide B	785.898	72.000 120.200	120	EGVNDNEEGFFSAR	+2	71.0	129.0 119.0

Chapter 4 - Results and Discussion

Nowadays, quantitative information of the expressed proteins is needed and constitutes a key-step to completely understand functions of organelles, cells, organisms as well as biochemical processes of modern society diseases. For this purpose, approaches for rapid, highly reproducible and accurate quantification of therapeutic proteins are crucial (95).

There is a large interest of COMT quantification due to its association with several neurological diseases. This work aims to develop a rapid, inexpensive, sensitive and accurate method capable of quantifying both COMT isoforms in complex samples. Thus, it was developed and applied a MRM method. Therefore, it was required to produce the COMT protein recombinantly and purifies it in order to create a COMT standard. Subsequently, this target fraction should be used in the calibration curves in order to determine quantitatively the COMT protein in complex samples such as cell lysates.

4.1. Production and purification of hSCOMT-His6

The first part of this work involved hSCOMT production and purification.

To obtain hSCOMT it was applied the same conditions previously described (53), since their production has succeeded in a *Pichia pastoris* expression system, using as a construct the plasmid pICZαA-hSCOMT_His6. In this approach, the protein is produced with a hexahistidine in its carboxyl-terminal, which will facilitate subsequent purification. Typically, *P. pastoris* have the capacity to secrete soluble proteins, however our target protein was retained intracellularly. Indeed, SDS-PAGE and western blot analysis indicate the presence of hSCOMT in the lysis pellet (Figure 9).

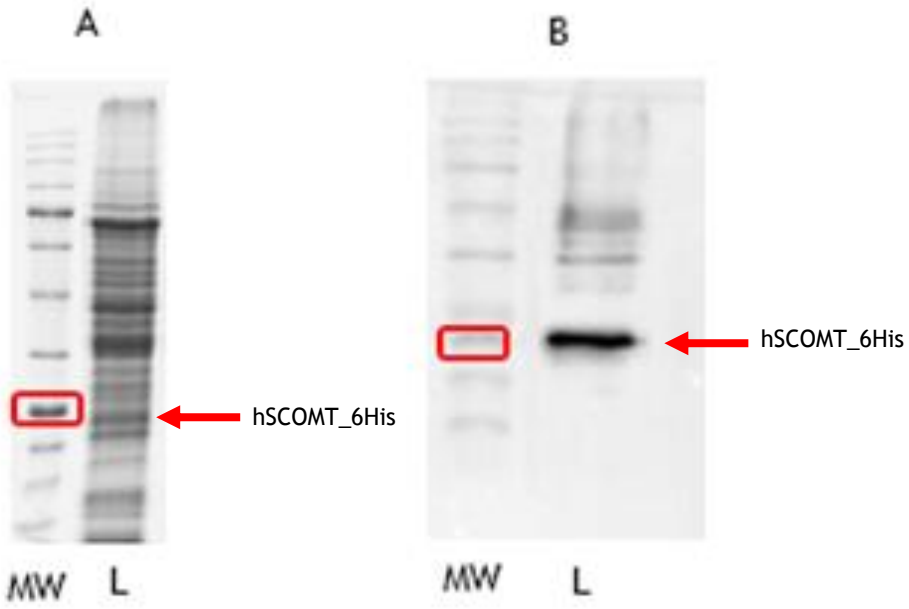

Figure 9 - SDS-PAGE (A) and Western-blot (B) analysis shows of the hSCOMT presence in crude *P. pastoris* lysates. MW – molecular weight standards; L – lysis pellet. The molecular weight of 25 kDa is indicated by red box and human SCOMT position by the red arrow.

Protein purification is carried out in two steps. First, an Immobilized Metal Affinity Chromatography (IMAC) was used with the same conditions earlier described in section 3.2.3. (53) with a different purpose of creating a COMT standard. This strategy was used because it was proved to be exceptionally efficient and selective for the isolation of hexahistidine tagged SCOMT.

As was described, the protein of interest is eluted with 300 mmol L^{-1} imidazole in a stepwise gradient previously optimized (53) (Figure 10). This behaviour, this was confirmed by SDS-PAGE and western- blot analysis (Figure 11).

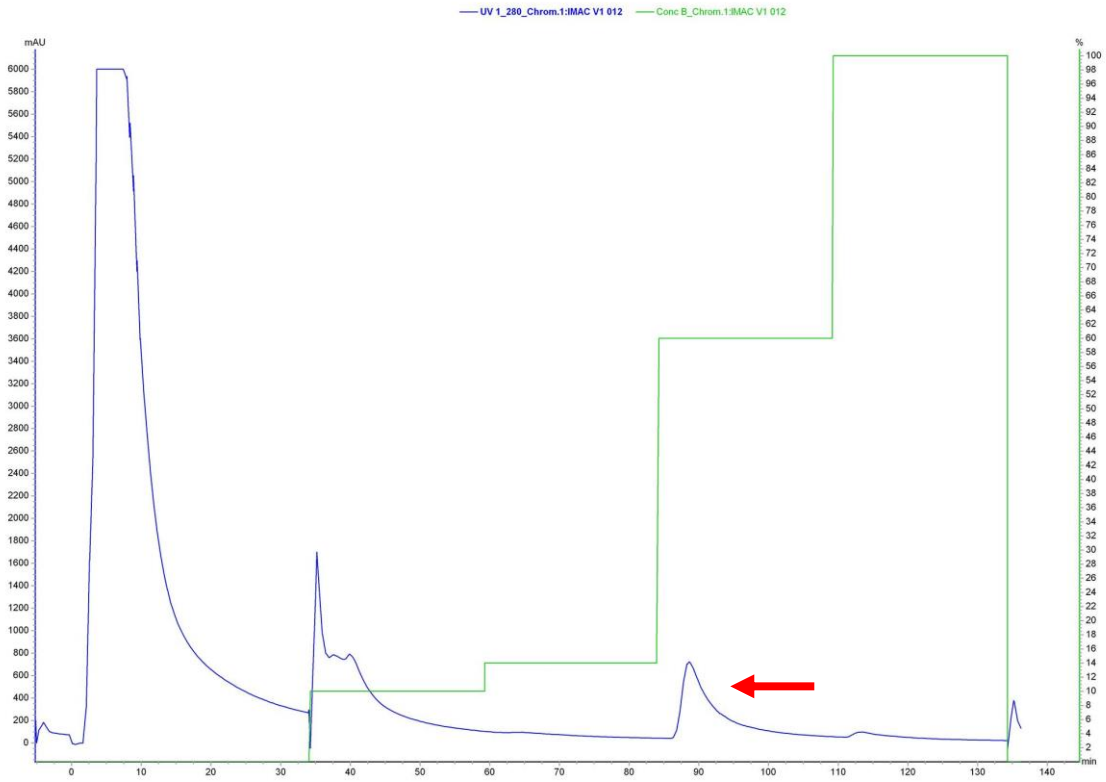

Figure 11 - A typical chromatographic profile of SCOM_6His by HisTrap HP 5mL with 2 mL loop and flow of 1 ml min^{-1}. Absorption was made with 500 mmol L^{-1} NaCl, 50 mmol L^{-1} Tris, 1 mmol L^{-1} $MgCl_2$, and 1 mmol L^{-1} imidazole, pH 7.8. Elution by stepwise gradient of 0%, 10%, 14%, 60% and 100% of imidazole in the buffer composes: 500 mmol L^{-1} NaCl, 50 mmol L^{-1} Tris, 1 mmol L^{-1} $MgCl_2$ and 500 mmol L^{-1} imidazole, pH 7.8. The peak elution of COMT is indicated by the red arrow.

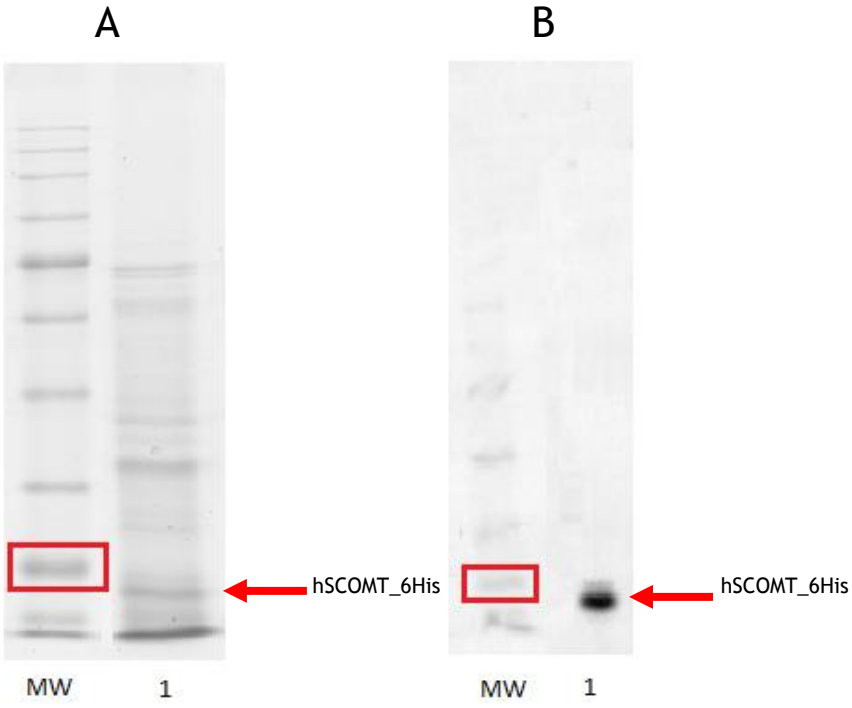

Figure 10 - SDS-PAGE 15% (A) and Western blot analysis (B) of samples collected on chromatographic profile of figure 10. MW – molecular weight standards; 1 – fraction obtained at 300 mmol L^{-1} imidazole. The molecular weight of 25 kDa is indicated by red box and human SCOMT position by the red arrow.

A completely purified protein is essential to develop a standard compound. However, as we can be seen by SDS-PAGE, the fraction obtained from IMAC was not entirely purified, an additional "purification" was used. This was done through the fractionation of the COMT band in SDS-PAGE gel. To make sure that there was no additional band of a different protein superimposed on the COMT band, the SDS gel was done with 15% acrylamide to increase the degree of separation of the proteins of lower molecular weight. After cutting the COMT band, the protein was extracted from the gel and digested for subsequent analysis by LC-MS/MS.

4.2. Peptide and MRM transition selection

Skyline is a platform for targeted proteomics method creation and quantitative data analysis. Skyline digests proteins and fragments peptides *in silico* to support direct peptide, precursor and transition picking, as well as automated picking using filters or spectral libraries, simplifying the development of mass spectrometry method (85).

Firstly, it was started by selecting peptides of COMT protein. In the literature is recommended the choice of 2 or more peptides per protein for quantitative analysis (74). *In silico* digestion given by Skyline (91) yielded 19 peptides, of which only 2 were chosen. Peptides containing cysteine were excluded immediately. However, it was not possible to avoid all the rejection conditions. Therefore, one of the chosen peptides have a methionine and histidine, subject to be modified. The exclusion reasons of each peptide are mentioned in the Table 3. The first 50 residues that are underlined are exclusive of a protein in membrane form. Since the chosen peptides are common to both COMT isoforms, this method can be used to quantify the two conformations. In addition, it is possible to use the method in the polymorphism Val/Met, because the chosen peptides do not contain the residue 158 (MBCOMT) or 108 (SCOMT).

Table 3 - The exclusion reasons applied of each COMT peptide. The chosen peptides are underlined.

sp|P21964|COMT_HUMAN	**Residues**		**Exclusion reasons**
-.MPEAPPLLLAAVLLGLVLLVVLLLLLR.H	[0 to 26]	X	• Spectrum information unavailable. • Containing glutamate.
R.HWGWGLCLIGWNEFILQPIHNLLMGDTK.E	[27 to 54]	X	• Spectrum information unavailable. • Containing cysteine, methionine, glutamate, asparagine and histidine.
R.ILNHVLQHAEPGNAQSVLEAIDTYCEQK.E	[58 to 85]	X	• Containing cysteine, asparagine, glutamate and histidine.
K.EWAMNVGDK.K	[86 to 94]	X	• Spectrum information unavailable. • Containing methionine, asparagine and glutamate.
K.GK.I	[96 to 97]	X	• Spectrum information unavailable. • Undersized.

K.IVDAVIQEHQPSVLLELGAYCGYSAVR.M	[98 to 124]	X	• Containing cysteine, glutamate and histidine.
R.MAR.L	[125 to 127]	X	• Spectrum information unavailable. • Undersized. • Containing methionine.
R.LLSPGAR.L	[128 to 134]	X	• Spectrum information unavailable. • Undersize.
R.LITIEINPDCAAITQR.M	[135 to 150]	X	• Containing cysteine, asparagine and glutamate.
R.MVDFAGVK.D	[151 to 158]	X	• Spectrum information unavailable. • Undersized. • Containing methionine.
K.DK.V	[159 to 160]	X	• Spectrum information unavailable. • Undersized.
K.VTLVVGASQDIIPQLK.K	[161 to 176]	√	• ----------
K.YDVDTLDMVFLDHWK.D	[179 to 193]	√	• Containing methionine and histidine.
K.DR.Y	[194 to 195]	X	• Spectrum information unavailable. • Undersized.
R.YLPDTLLLEECGLLR.K	[196 to 210]	X	• Containing cysteine and glutamate.
K.GTVLLADNVICPGAPDFLAHVR.G	[212 to 233]	X	• Containing cysteine, asparagine and histidine.
R.GSSCFECTHYQSFLEYR.E	[234 to 250]	X	• Containing cysteine, glutamate and histidine.
R.EVVDGLEK.A	[251 to 258]	X	• Spectrum information unavailable. • Undersized. • Containing glutamate.
K.AIYK.G	[259 to 262]	X	• Spectrum information unavailable. • Undersized.
K.GPGSEAGP.-	[263 to 270]	X	• Spectrum information unavailable. • Undersized. • Containing glutamate.

After the choice of selected peptides, their MRM transition precursor (Q1) and fragment (Q2) ions were exported from Skyline (91) as well as the declustering potential and collision energy of each transition (see Table 4). Due to the existence of amino acids that are prone to modifications in one of the selected peptides, both the modified and the unmodified versions of the peptide were evaluated. The M(147) indicated oxidized methionine.

Table 4 - MRM transitions, declustering potential and collision energy precursor (Q1) of selected peptides exported from Skyline (91).

Q1	Q3	Ion type	ID	Charge	Declustering potential	Collision energy
840.998362	1169.652464	y11	VTLVVGASQDIIPQLK	+2	92.4	43.7
	485.308209	y4				
	413.275846	b4				
	1083.604451	b11				
	1196.688515	b12				
561.001333	598.392273	y5		+3	72	24.5
	485.308209	y4				
	413.275846	b4				
	512.34426	b5				
	640.402838	b7				
948.945469	1190.566291	y9	YDVDTLDMVFLDHWK	+2	100.3	49.8
	1075.539348	y8				
	845.43045	y6				
	585.277972	y4				
	470.251029	y3				
632.966071	845.43045	y6		+3	77.3	26.7
	279.097548	b2				
956.942927	1420.692949	y11	YDVDTLDM(147)VFLDHWK	+2	100.9	50.3
	1206.561206	y9				
	1091.534263	y8				
	845.43045	y6				
	698.362036	y5				
638.29771	585.277972	y4		+3	77.6	6.9
	279.097548	b2				
	493.192905	b4				

The transitions exported from the Skyline (91) were evaluated by injecting 5 µL of a digested SCOMT (300 fmol μL^{-1}) in the equipment through a separation provided by an HPLC system on Synergi 4U Fusion-RP 80A column. Chromatography is used to fractionate tryptic peptides derived from a protein sample before ionization and injection into the mass spectrometer. In these first evaluations it was developed and optimized a HPLC method in order to extend 30 min the run cycle to evaluate the peptides behaviour. The mobile phases used were (A) 0.1% formic acid in water and (B) 0.1% formic acid in acetonitrile at a flow rate of 100 µL min^{-1}. The HPLC method started with column equilibration for 2 min at 2% B, followed by a linear gradient of 30% to 80% B from 2 to 20 min and an isocratic step at 80% B for 4 min. Finally, a linear step of 80% to 3% B during 2 min and then the column was equilibrated again at 2% B for 4 min. The 4000 QTrap instrument source parameters were ion spray voltage at 5500 V, the heater gas temperature at 0 ºC, a nebulizer gas (GS1) of 60 Pa, a heater gas (GS2) of 60 Pa and a curtain gas of 20 Pa. These parameters were chosen considering the published papers (93, 94) in this area and were subsequently optimized. The result of the SCOMT standard injection was compared with a blank sample injection using the same method (see Figure 12).

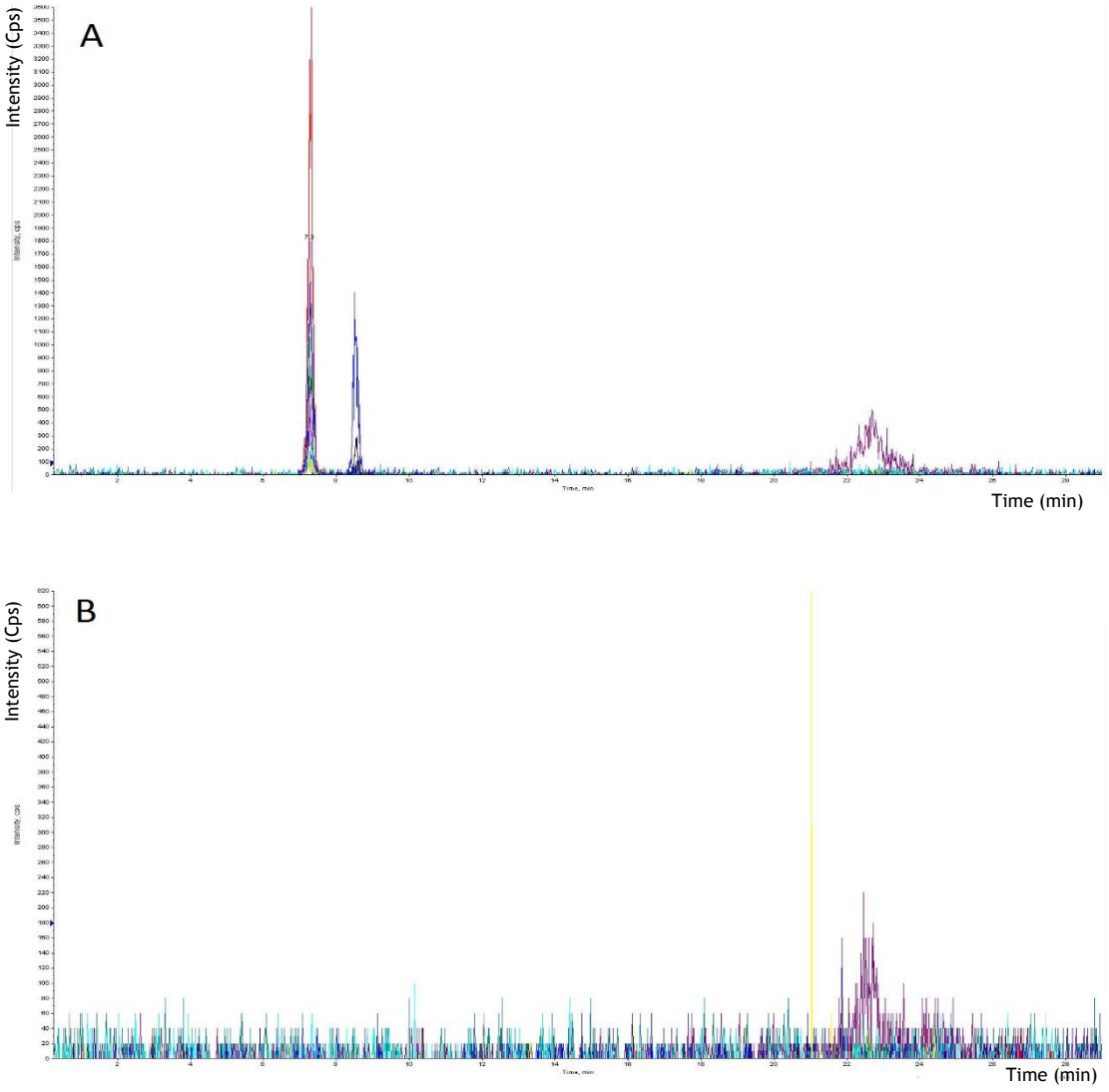

Figure 12 - Chromatograms obtained after analysis of SCOMT (A) and blank sample (H_2O + 1% AF) (B).

As seen in the spectrum, all transitions of the peptide VTLVVGASQDIIPQLK appear at the same retention time, confirming that are all part of the same peptide. The peptide VTLVVGASQDIIPQLK has a retention time around 7 minutes and provides a much higher signal than peptide YDVDTLDMVFLDHWK. The transition 840.998/485.308 showed the highest signal, being chosen to be used in the protein quantification. The transitions that followed with best signal were 840.998/1196.688 and 840.998/413.275, showing that the peptide mainly acquires charge +2 during the ionization. According to SRM collider (92), these three transitions combined are specific for COMT (Figure 13), so they were selected for the quantification method. SRM collider is a tool that helps in the creation of specific SRM assays for peptide, comparing our input transitions to all other transitions in a given background proteome and find specific interferences (96).

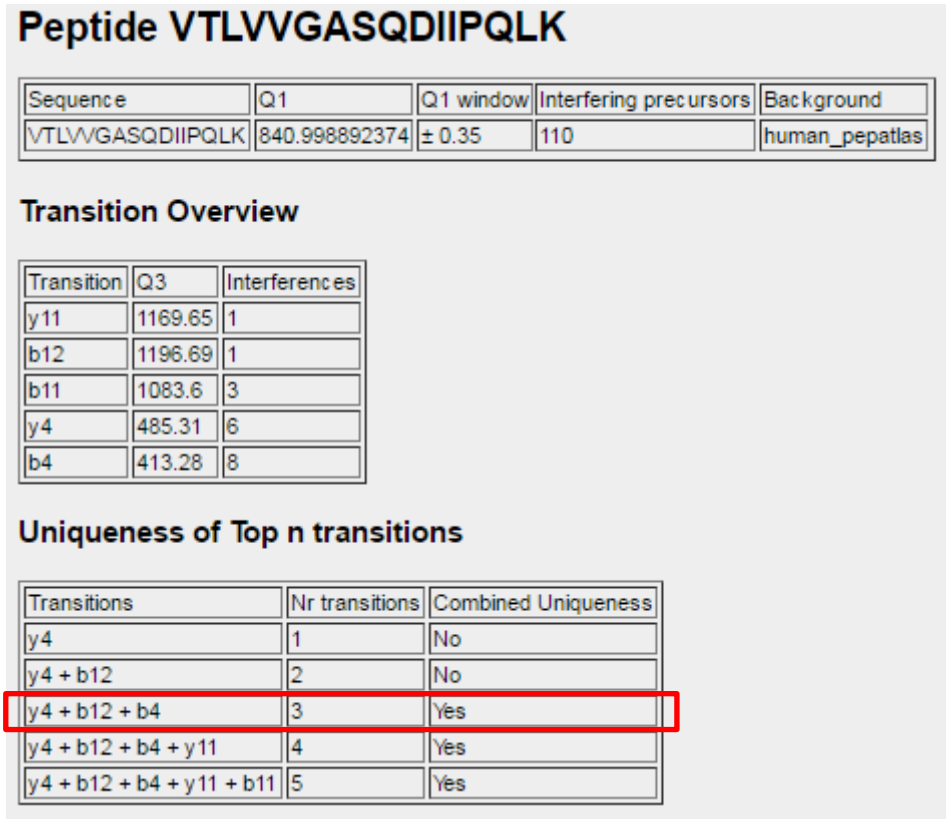

Peptide VTLVVGASQDIIPQLK

Sequence	Q1	Q1 window	Interfering precursors	Background
VTLVVGASQDIIPQLK	840.998892374	± 0.35	110	human_pepatlas

Transition Overview

Transition	Q3	Interferences
y11	1169.65	1
b12	1196.69	1
b11	1083.6	3
y4	485.31	6
b4	413.28	8

Uniqueness of Top n transitions

Transitions	Nr transitions	Combined Uniqueness
y4	1	No
y4 + b12	2	No
y4 + b12 + b4	3	Yes
y4 + b12 + b4 + y11	4	Yes
y4 + b12 + b4 + y11 + b11	5	Yes

Figure 13 - The SMR Collider results for the ion precursor 840.998. The red box indicates the minimum combined transitions to achieve uniqueness in human Peptide Atlas background (92).

On the other hand, the peptide YDVDTLDMVFLDHWK is eluted around 8 minutes and seems to acquire mostly charge +3. Transitions associated with the modified peptide showed much smaller signals than transitions without methionine modification. So, since the peptide does not appear to undergo modification, these transitions were discarded. The best transitions of this peptide showed to be 632.966/845.430 and 632.966/279.097 and were incorporated in the method. This peptide will only serve to confirm the existence of COMT protein in

combination with peptide VTLVVGASQDIIPQLK, and it will not be used for quantification procedures.

Typically, the incorporation of controls during sample preparation can be useful in order to track analytical, chromatography and sample preparation variability and reproducibility (74). In this work, it was used the Glu1-Fibrinopetide B as an internal control. To discover their MRM transitions and optimal conditions, the Glu1-Fibrinopetide B (500 fmol μL^{-1}) was infused with mobile phase at a flow-rate of 20 µL min^{-1} using a syringe pump. The search range was 500 to 1500 Da and the final method was build using 5 most intense peaks from the most 20 peaks. Infusion is the continuous flow of the sample at low flow rates into the ion source using a syringe pump. During the infusion optimization process, the software can select precursor and production ions and optimize for declustering potential and collision energy. So, the obtained conditions (DP and CE) from Glu1-Fibrinopetide B infusion are described in Table 5.

Table 5 - Conditions (DP and CE) of Glu1-Fibrinopetide B obtained from infusion optimization.

Q1	Q3	Dwell	ID	Charge	Declustering potential	Collision energy
785.898	72.0	120	EGVNDNEEGFFSAR	+2	71	129.0
	120.2					119.0
	70.1					129.0
	84.0					129.0
	684.9					51.0

The Glu1-Fibrinopetide B transitions were evaluated by injecting 5 µL of a commercial Glu1-Fibrinopetide B standard (250 fmol μL^{-1}) in the equipment 4000 QTrap through a separation by an HPLC system with the same method (20 min) described above. The spectrum of the Glu1-Fibrinopetide B was compared with a blank sample injection using the same method (see Figure 14).

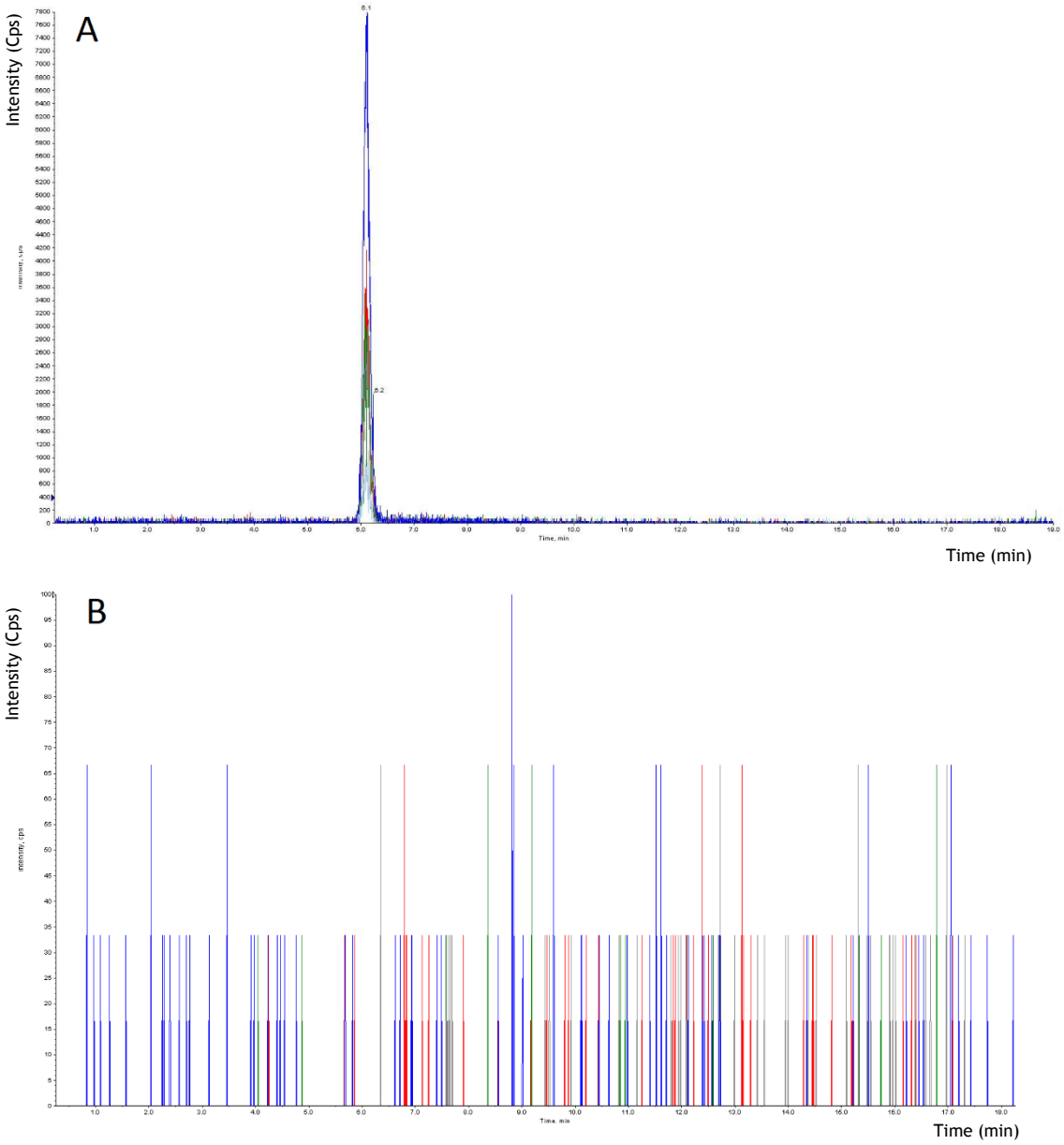

Figure 14 - Chromatograms obtained after analysis of Glu1-Fibrinopeptide B at 500 fmol μL^{-1} (A) and blank sample (H_2O + 1% AF) (B).

The results show that, Glu1-Fibrinopetide B has a retention time around 6 minutes, which does not interfere with the retention time of COMT peptides, so it can be used as an internal control. The best transition with the highest signal were 785.898/72.0 and 785.898/120.2. So, both were incorporated in the method.

4.3. Method optimization

4.3.1. High-performance liquid chromatography (HPLC)

Initially, the HPLC method had a duration of 30 minutes, which was shortened to 20 minutes, since the peptides showed retention time between 6 and 8 minutes. Therefore, the method was also started with column equilibration for 2 min at 2% B, followed by a linear step of 30% to 80% B from 2 to 10 min. Then, an isocratic gradient was applied at 80% B for 4 min and a linear step of 80% to 3% B during 2 min. At the end, a new column equilibration was obtained at 2% B for 4 min.

4.3.2. Source parameter

Source parameters are settings that control the electrospray ionization and tend to be constant from day-to-day, but they can differ progressively over time (70).

To determine the source parameter settings, a peptide standard, such as Glu1-Fibrinopeptide B, can be used. The parameters can be adjusted in order to optimize the signal strength. To optimize the source parameters, 5 µL of Glu1-Fibrinopeptide B with 500 fmol μL^{-1} were used for each injection. All the injections were performed twice. The signal presented is the average of two injections per parameter.

4.3.2.1. Temperature

The temperature is used to evaporate the sample. The ideal temperature is the lowest temperature at which the sample is vaporized completely (74, 83).

If the temperature is set too low, then the vaporization is incomplete and large, visible droplets are expelled into the ion source housing. If the temperature is set too high, the solvent may vaporize prematurely. At higher flow rates the optimal temperature increases.

Normal optimization is usually performed with increments of 50 ºC and it should be adjusted to achieve the best signal or signal-to noise ratio. At LC flow 100 µL min^{-1}, the typical temperature values are between 450 ºC and 650 ºC. In this work, the temperatures tested were 0, 450, 500, 550, 600, 650, 700 and 750 ºC, and the signal value obtained for each one is shown in Table 6. The displayed value is an average of the two injections per temperature value. When the temperature ranges between 450 ºC and 650 ºC, the obtained signal was identical. The signal takes its maximum value at 550 ºC.

Table 6 – Signal value obtained at each temperature.

Temperature (ºC)	Signal (cps)
0	$7.10 \times 10^3 \pm 989.9$
450	$2.10 \times 10^4 \pm 1414.2$
500	$2.10 \times 10^4 \pm 0.0$
550	$2.20 \times 10^4 \pm 707.1$
600	$2.10 \times 10^4 \pm 0.0$
650	$2.10 \times 10^4 \pm 707.1$
700	$1.95 \times 10^4 \pm 707.1$
750	$1.60 \times 10^4 \pm 707.1$

4.3.2.2. IonSpray voltage

The IonSpray parameter is the voltage applied to the sprayer, which ionizes the sample in the ion source. This parameter depends on the polarity, and affects the sensitivity and stability of the spray (74, 83).

The optimum IonSpray voltage is the lowest value possible without losing signal and the typical range is 4500 V to 5500 V (94). the IonSpray voltage tested were 5500, 5000, 4500, 4000 and 3000 V, and the signal value obtained for each one is shown in Table 7. The displayed value is an average of two injections per IonSpray value. The best signal was obtained at 5000 V, so this was the optimum IonSpray voltage. This optimization has been made based on the previous results obtained at temperature of 550 ºC.

Table 7 - Signal value obtained at each IonSpray voltage.

IonSpray (V)	Signal (cps)
5500	$2.10 \times 10^4 \pm 0.0$
5000	$2.25 \times 10^4 \pm 707.1$
4500	$2.05 \times 10^4 \pm 0.0$
4000	$1.50 \times 10^4 \pm 707.1$
3000	$4.40 \times 10^3 \pm 70.7$

4.3.2.3. Nebulizer gas (GS1) and heater gas (GS 2)

Nebulizer gas (GS1) helps to produce small droplets of sample flow, while heater gas (Gas 2) aids in the evaporation of solvent (74).

Optimization of these two parameters should be adjusted to achieve the best signal stability and sensitivity. Too high heater gas can cause premature vaporization of the solvent, which will result in the instability of the signal and a high chemical background noise (70). A value between 40 and 60 Pa for GS1 was used as well as a value between 30 and 50 Pa for GS2.

In this optimization, a fixed value of 30 Pa for GS2 was typed for the optimization of GS1 and the values tested were 40, 50, 60, 70, 80 and 90 Pa. For the GS2 optimization, a fixed value of 80 Pa was set for GS1 the optimal value and the values tested were 30, 40, 50, 60 and 70 Pa. The signal obtained from GS1 and GS2 are shown in the Table 8 and Table 9, respectively. The displayed value is an average of two injections per gas value. The best signal obtained for GS1 was at 80 Pa and for GS2 was at 50 and 60 Pa. Thus, the optimal value obtained for GS1 was 80 Pa and the value chosen for GS2 was the 50 Pa, since it is the most common described in the literature (93).

Table 8 - Signal value obtained at each GS1 measure.

GS1 (Pa)	Signal (cps)
40	$1.65 \times 10^4 \pm 707.1$
50	$1.80 \times 10^4 \pm 0.0$
60	$2.00 \times 10^4 \pm 0.0$
70	$2.10 \times 10^4 \pm 0.0$
80	$2.15 \times 10^4 \pm 2121.3$
90	$2.10 \times 10^4 \pm 707.1$

Table 9 - Signal value obtained at each GS1 measure.

GS2 (Pa)	Signal (cps)
30	$2.10 \times 10^4 \pm 0.0$
40	$2.10 \times 10^4 \pm 707.1$
50	$2.20 \times 10^4 \pm 0.0$
60	$2.20 \times 10^4 \pm 707.1$
70	$2.10 \times 10^4 \pm 0.0$

4.3.2.4. Curtain gas (CUR)

Typically, curtain gas helps to prevent contamination of the orifice while permitting direction of sample ions into the vacuum chamber by the electrical fields generated between the vacuum interface and the spray needle. Contamination of the ion entrance optics reduces Q0 transmission, stability, and sensitivity, and increases background noise (70, 74).

It should be maintained as high as possible without losing sensitivity and decreasing the signal. CUR should never be less than 20 Pa to avoid possible contamination. CUR values tested were 20, 25, 30, 35 and 40 Pa. The signal obtained for each value is shown in Table 10. The displayed value is an average of two injections per gas value. By increasing the CUR value led to a decreasing in the signal value. As a result, the minimum value for CUR was settled to 20 Pa.

Table 10 - Signal value obtained at each curtain gas measure.

CUR (Pa)	Signal (cps)
20	$2.7 \times 10^4 \pm 1414.2$
25	$2.65 \times 10^4 \pm 707.1$
30	$2.55 \times 10^4 \pm 707.1$
35	$2.4 \times 10^4 \pm 1414.2$
40	$2.3 \times 10^4 \pm 707.1$

4.3.3. Compound parameter

Due to the lack of available COMT sample, the optimization of the source- dependent parameter, such as CE and DP, was done through the FIA compound optimization.

Flow Injection Analysis (FIA) is the injection of a small quantity of a sample by the autosampler into the mass spectrometer using LC. FIA compound optimization can optimize the compound- and the ion source- dependent parameter. In contrast to the ion source parameters, which require one injection per value per replicate, compound-dependent parameters only require one injection per parameter, so it is possible to reduce the sample application. In FIA, the optimizations are made for each pre-set Q1/Q3 transition. CE values tested were 20, 30, 40, 50, 60, 70, 80, 90, 100 and 110. The optimized transitions were 840.998/485.308, 840.998/1196.688 and 840.998/413.275. The transitions 632.966/845.430 and 632.966/279.097 were not optimized due to the low intensity. For DP, the values verified were 60, 70, 80, 90, 100, 110. 120, 130, 140 and 150. The optimal value obtained for DP was 120 and for CE was 50, both for all evaluated transitions.

4.4. Method validation

The objective of validation of an analytical procedure is to demonstrate that it is suitable for its intended purpose. A full validation is important when developing and implementing a bioanalytical method for the first time.

The method was validated according to international guidelines from the Food and Drug Administration (FDA) (97) and International Conference on Harmonization (ICH) (98). The evaluated parameters included selectivity, linearity, precision and accuracy, limit of detection (LOD), limit of quantification (LOQ), carry-over and matrix effects. Only the transition 840.998/485.308 was evaluated in the parameters with the exception of selectivity, where were evaluated the 840.998/485.308, 840.998/1196.688 and 840.998/413.275.

4.4.1. Selectivity

Selectivity is the capacity of the method to quantity and differentiate the analytes from any other components present in the sample. These could include metabolites, impurities, degradants or matrix components (97).

This parameter was evaluated by using two blank matrixes which were spiked with SCOMT and IS and compared with two blank matrixes without the spike, not even with IS. The matrixes used were the mobile phase A and the digested lysate of *P. pastoris* X-33 without the plasmid pICZαA-hSCOMT_His6. The criteria used for the selectivity parameter were defined by the World Anti-Doping Agency (WADA) identification criteria for qualitative assays incorporating column chromatography and mass spectrometry (Table 11) (99). An absolute retention time (RT) within 2% (± 0.1 min) of the RT of three transitions of the analyte were assumed and the relative ion intensities between transitions a presented in Table 12.

Table 11 - Criteria of the relative abundance applied with different percentages of relative area (99).

Relative Abundance in the reference specimen (% of base peak)	**Maximum Tolerance Windows for the Relative Abundance in the Sample**
50 - 100	± 10 (absolute)
25 - 50	± 20% (relative)
1 - 25	± 5 (absolute)

Table 12 - Absolute area, relative abundance and retention time of transitions.

	Absolute area	**Relative abundance (%)**	**RT_A**	**RT_{IS}**
840.998/485.308	42630	100.0	6.83	6.11
840.998/1196.688	19400	45.5	6.83	6.11
840.998/413.275	11460	26.9	6.82	6.11

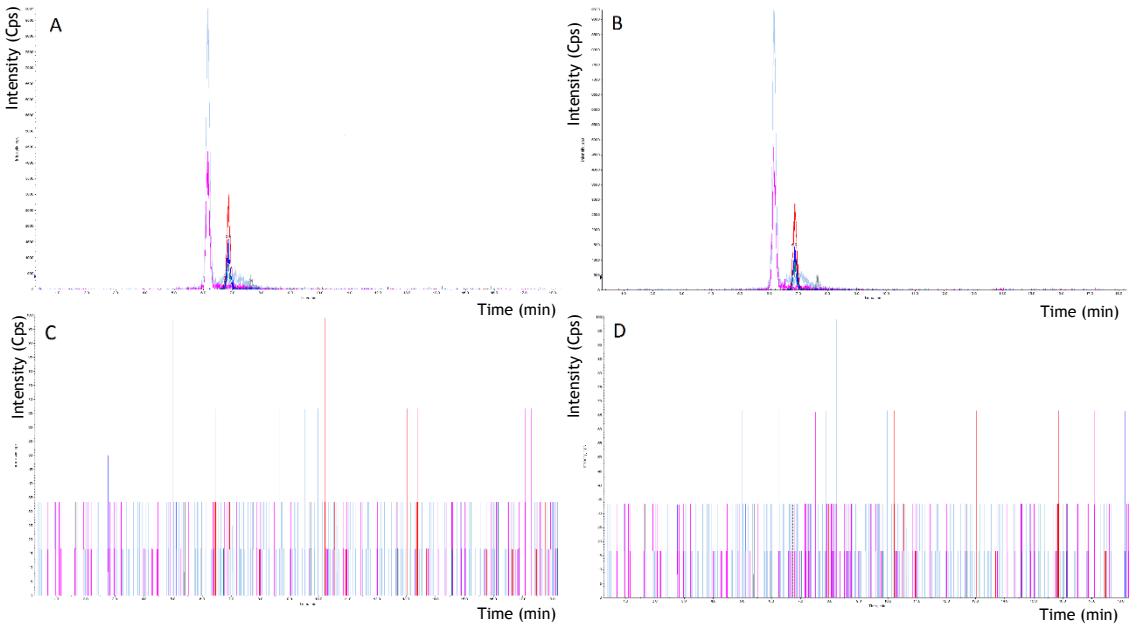

Figure 15 - Chromatograms obtained after analysis of blank sample matrixes spiked with SCOMT at 100 µg mL^{-1} and Glu1-Fibrinopeptide B at 150 fmol μL^{-1} (A)(B) and blank matrix without spike - mobile phase A (C); digested lysate (D).

By comparing the spiked samples with the blank samples (see Figure 15), according to the above described criteria, can be proved that the method is selective for the analyte since no signal overlay was found at retention times of the target analytes.

4.4.2. Linearity and limits of detection and quantification

Linearity is the ability to obtain test results that are directly proportional to the concentration of analyte in the sample. For the establishment of linearity, a minimum of 5 concentrations is recommended. Normally, the linearity is assessed graphically, in addition to mathematical evaluation. A curve that results from plotting the concentration of the standard versus the ratio of the peak area of the analyte and the peak area of the internal standard, given the equation $y = mx + b$, where m is the slope and the b is the y interception. Values over 0.99 are considered acceptable for the correlation coefficient (R) and the coefficient of determination (R^2) (46, 97).

To assess the linearity of the method, a calibration curves (n=5) with the working range of 25 to 200 µg mL^{-1} were prepared, in the concentrations of 25, 30, 50, 100 and 200 µg mL^{-1}. Every samples were spiked with 5 µL of Glu1-fibrinopeptide B 1350 fmol μL^{-1} (IS). The calibration curve results from plotting the concentration of the standard versus the ratio of the peak area of the analyte and the peak area of the internal standard.

Limit of detection (LOD) is the lowest amount of analyte in a sample which can be detected but not necessarily quantitated as an exact value and can be calculated by using the parameters of the calibration curve's equation by the equation (1). On the other hand, limit of quantitation (LOQ) is the lowest amount of analyte in a sample which can be quantitatively

determined with suitable precision and accuracy and can be calculated by the equation (2). The lowest standard on the calibration curve can also be accepted as the limit of quantification if the analyte response at the LLOQ (Lower Limit Of Quantification) was at least 5 times the response compared to blank response and reproducible with a precision of 20% and accuracy of 80-120% (97, 98).

$$LOD = \frac{3.3 \times S_{y/x}}{m} \quad (1)$$

$$LOQ = \frac{10 \times S_{y/x}}{m} \quad (2)$$

$S_{y/x}$ – Standard deviation of the linear correlation.
m – Slope of the calibration curve's equation.

A summary of the linearity results and limits is presented in Table 13. In addition, a linear regression equation applied to the results is represented graphically in the following Figure 16.

In terms of the criteria applied to the classical linear regression, the calibration curve fulfilled such criteria, with every R^2 value above 0.99 and a confidence interval containing zero. The lowest standard used on the calibration curve fulfils the criteria described above to be accepted as the limit of quantification. In conclusion, the method was found to be linear in the studied range of 25 to 200 µg mL^{-1}. Since in the literature there is no published work to our knowledge that contain these parameters for COMT protein, it is not possible to compare our results.

Table 13 - Linearity data and limits (n=5).

Calibration rage (µg mL^{-1})	**Calibration curve**		**R^2**	**$S_{y/x}$**	**LLOQ (µg mL^{-1})**	**LOD (µg mL^{-1})**
25 - 200	m 0.0036 ± 0.0007	b -0.0894 ± 0.0215	0.9979 ± 0.0041	0.0036 ± 0.0018	25	3,3

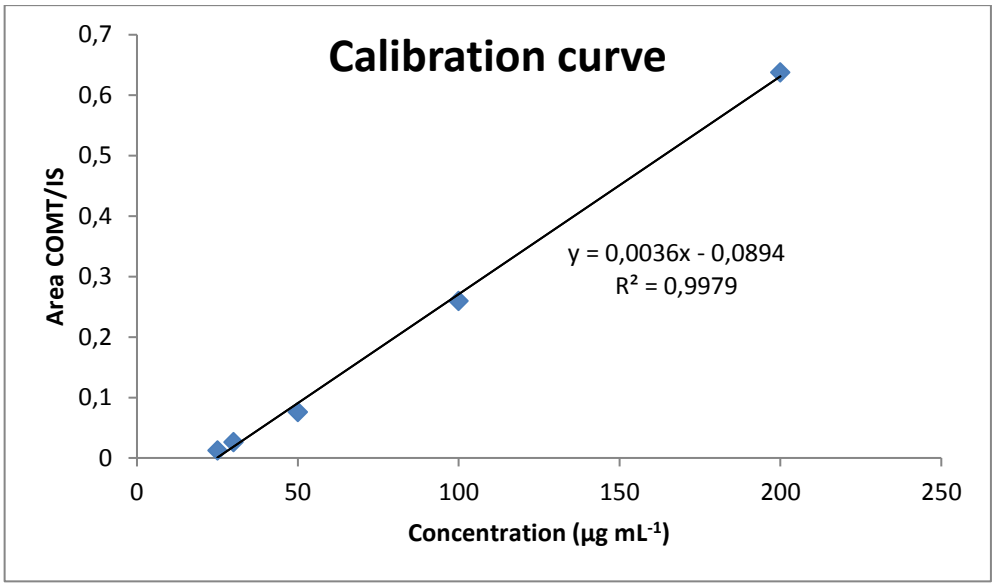

Figure 16 - Graphical example of a calibration curve.

4.4.3. Precision and accuracy

The precision of an analytical method describes the closeness of individual measures of an analyte when the procedure is applied repeatedly (97). The within-run precision expresses the precision under the same operating conditions over a short interval of time, which was calculated by the equation (3). The precision determined at each concentration level should not exceed 15% of the coefficient of variation (CV) except for the LLOQ, where it should not exceed 20% of the CV (97, 98, 100).

The accuracy of an analytical method expresses the closeness of mean test results obtained by the method to the true value (concentration) of the analyte. The deviation of the mean from the true value serves as the measure of accuracy, which is expressed in %RE, being calculated by the equation (4). Like precision, the mean value should be within 15% of the actual value except at LLOQ, which should not diverge more than 20% (97, 98, 100).

The precision and accuracy of a method should be measured using at least three concentrations of the calibration range (including the highest and lowest concentration) and at least five determinations for each concentration (97). Within-run precision and accuracy were evaluated by analysing different concentration in 5 replicates during the same day (n=5). The working range was the same as was used for linear assessment (section 4.4.2) as well as the spiked with 5 µL of Glu1-fibrinopeptide B 1350 fmol µL^{-1} (101).

$$\%\ CV\ Repeatability\ within = \frac{\sqrt{S^2_{within}}}{\bar{x}} \times 100$$

S^2_{within}- Variance between groups.

$\bar{x}$ - Average of measurements.

$$\%RE\ Accurancy = \frac{C_{obs} - C_{real}}{C_{real}} \times 100 \qquad (4)$$

C_{obs} – Observed concentration.

C_{real} – Real concentration.

The within-run precision and accuracy are shown in Table 14. Both evaluated parameters were found acceptable according to the guidelines. The values are within ± 15%, except at LLOQ, where are not deviate by more than ± 20%.

Table 14 - Within-run precision and accuracy (n=5).

Concentration (µg mL^{-1})	Measured concentration (µg mL^{-1})	CV (%)	RE (%)
25	28.00 ± 1.09	19.60	11.99
30	31.28 ± 1.49	8.88	4.28
50	45.72 ± 5.01	5.51	-8,.56
100	106.41 ± 3.17	7.96	6.41
200	220.38 ± 6.65	14.80	10.19

4.4.4. Carry-over

Carry-over is the presence of analyte signal in blank samples after the analysis of target samples and it is a major problem that can influence the accuracy and precision of LC-MS/MS bioanalysis (98). The carry-over effect was evaluated by injecting blanks after the samples and analysing if the signal from the previously injected sample is present. For this purpose, three replicates of the highest calibrator (200 µg mL^{-1}) were injected each followed by the injection of three blanks, which consisted of mobile phase A (H_2O + 0.1% formic acid) used.

Carry-over in the blank sample following a high concentration standard should not be greater than 20% of the LLOQ and 5% for the IS. As can be seen in Figure 17, which display the mean results obtained, there was no carry-over effect observed since it does not appear any response in the chromatograms of the injected blank samples following the standard samples injection.

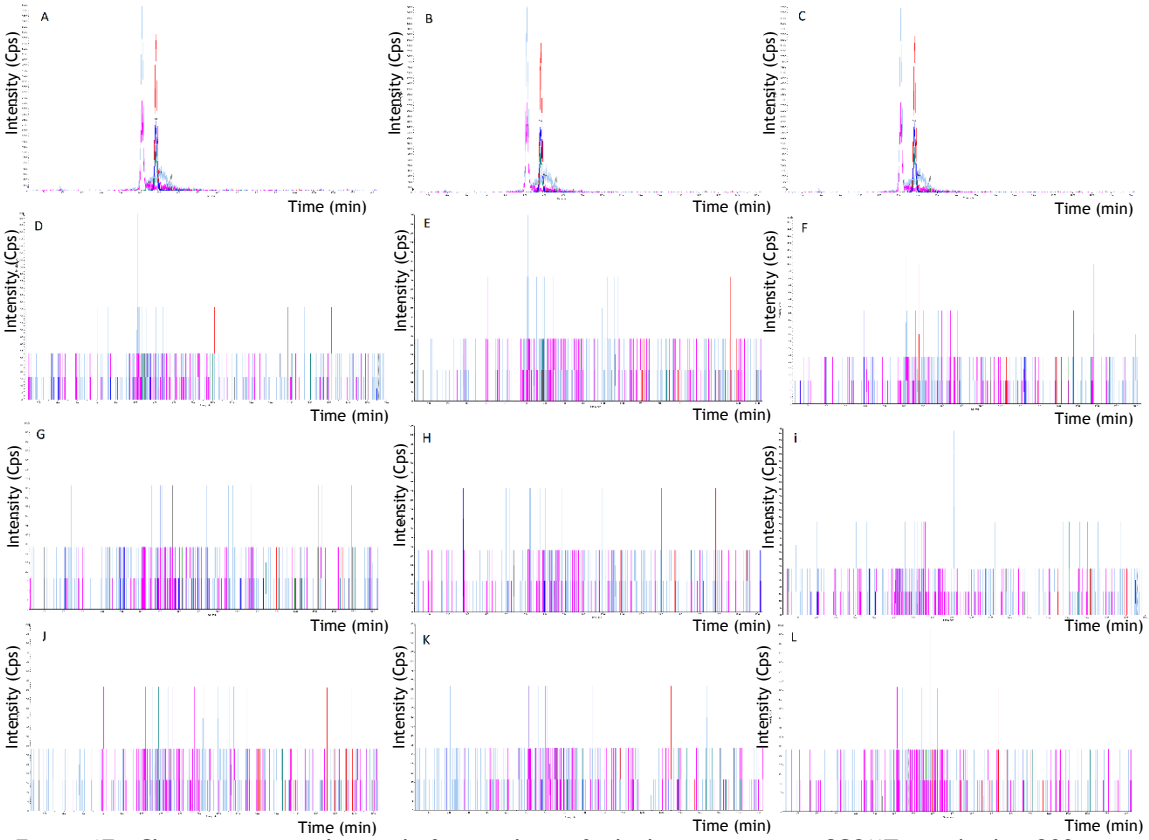

Figure 17 - Chromatograms obtained after analysis of a high concentration SCOMT standard at 200 µg mL^{-1} with Glu1-Fibrinopeptide B at 150 fmol μL^{-1} (A)(B)(C) and blank samples (D)(F)(G)(H)(I)(J)(K)(L).

4.4.5. Matrix effects

Matrix effects may cause a different compound's response when the analyte was analysed in a biological matrix compared to a standard solution. The difference can be described as suppression or enhancement of response, since the matrix compounds can influence the analyte ionization (100).

The matrix effects were measured by comparing the peaks areas of the analyte of interest spiked to blank matrix extracts with different origins in two different concentrations and injected in triplicate. The matrixes used were the mobile phase A and the digested lysate of *P. pastoris* X-33 without the plasmid pICZαA-hSCOMT_His6. Both matrixes were spiked with the same amount of SCOMT. Matrix effects can be expressed in terms of matrix influence factor f, which is measured by the equation (5) (100).

$$f = \frac{A_{matrix} - A_{pure\ standard}}{A_{pure\ standard}} \qquad (5)$$

A_{matrix}- Peak area of the analyte obtained by spiking a blank matrix extracts.

$A_{pure\ standard}$ – Peak area of the analyte as pure reference standard solution.

Using the formula (5), f = 0 would represent no matrix effects, a negative value indicates ion suppression and a positive one ion enhancement (100). As the criteria for the study of matrix effects, the coefficient of variation calculated from f should be lower than 15% when multiplied by 100 (100). The results are shown in Table 15. The matrix effects were found not to be significant, showing all values near 0. Additionally, this effect may be visually evaluated by comparing the chromatograms obtained from the analysis of the analyte in mobile phase A and in digested lysate of *P. pastoris* X-33 without the plasmid pICZαA-hSCOMT_His6. In this samples, it is observable a remarkable similarity between both chromatograms, in mobile phase A and in digested lysate (Figure 18).

Table 15 - Matrix effects at two different COMT dilution (200 µg mL^{-1} and 100 µg mL^{-1}).

		f
COMT	200 µg mL^{-1}	0.0311
	100 µg mL^{-1}	0.0222
GF	150 fmol μL^{-1}	0.0915
	75 fmol μL^{-1}	0.0256

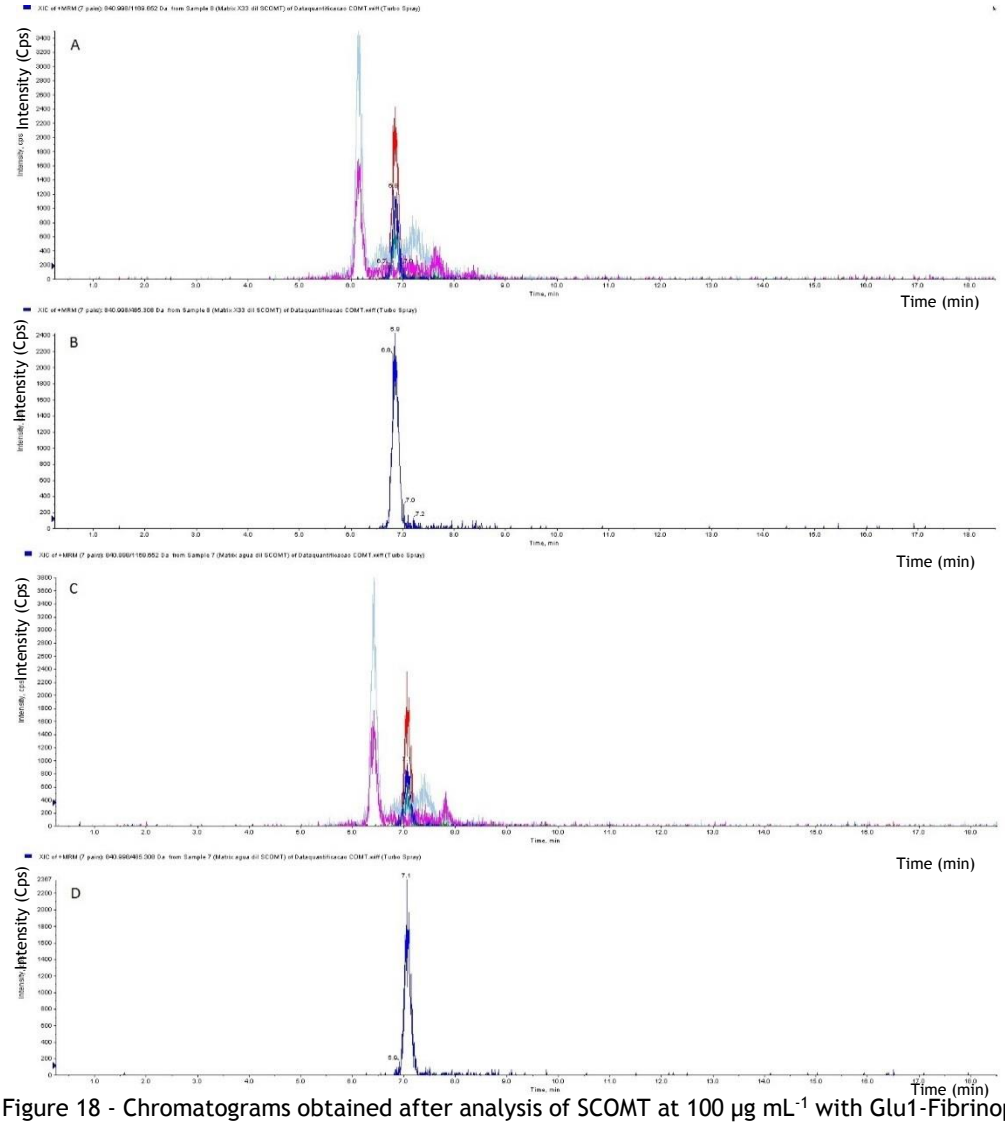

Figure 18 - Chromatograms obtained after analysis of SCOMT at 100 µg mL^{-1} with Glu1-Fibrinopeptide B at 150 fmol μL^{-1} spiked in mobile phase A (A) and in digested lysate (C). The chromatograms (B) and (D) show the extract 840.998/485.308 ions from the chromatograms (A) and (C), respectively.

4.5. Quantification of COMT isoforms in *Pichia pastoris* lysates

As already mentioned, this method is feasible in both COMT isoforms, since the peptide used to quantify is common to both isoforms. Thus, the method was used for SCOMT and MBCOMT quantification, both in complex media such as cell lysates (Figure 19). The proteins were produced and in-solution digested as described in section 3.2.2 and 3.2.7., respectively, and prepared as described in section 3.2.9. The concentration of unknown SCOMT and MBCOMT samples was calculated by the regression equation generated by one calibration curve with the working range of 25 to 200 µg mL^{-1}. Every concentration was spiked with 5 µL of Glu1-fibrinopeptide B 1350 fmol $µL^{-1}$ (IS). This calibration curve was generated on the same day when the measurements of samples were made. Each unknown sample injection was performed in triplicate. The average of calculated concentrations of SCOMT and MBCOMT were 62.35 ± 3.73 and 58.69 ± 1.49 µg mL^{-1}, respectively. The values obtained in each measurement were within the calibration curve values, showing that the range used fits in the type of samples to quantify. Finally, the applicability of the method in complex samples was proved.

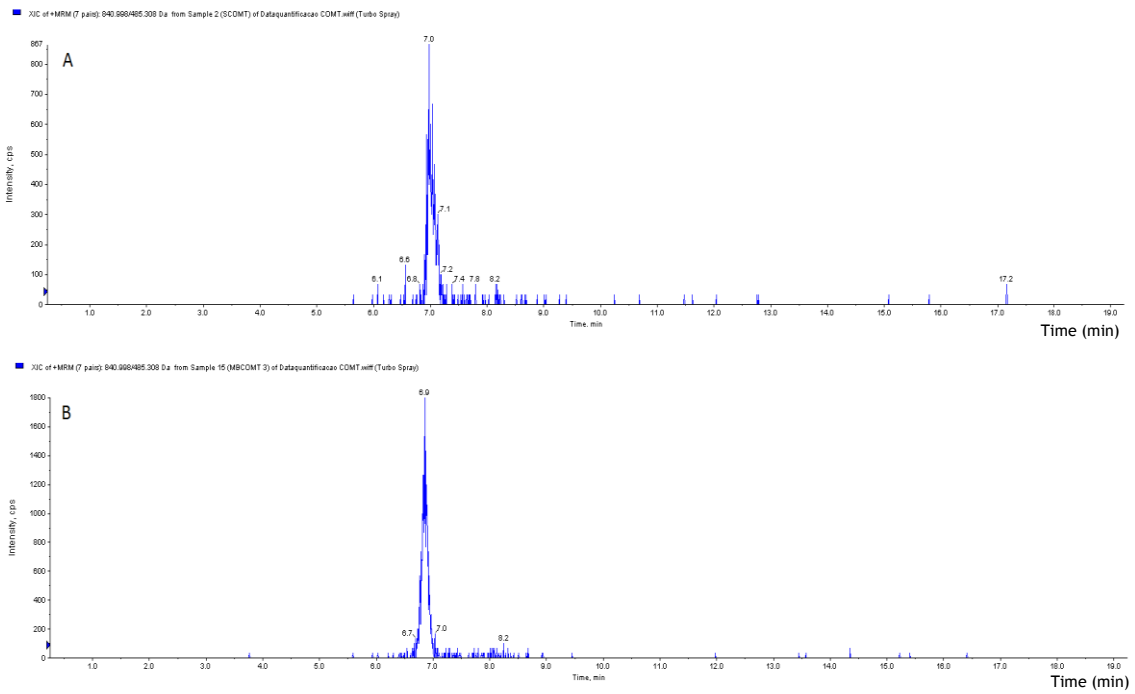

Figure 19 - Chromatograms obtained by the extract 840.998/485.308 ions after analysis of unknown SCOMT (A) and MBCOMT (B) in digested *P. pastoris* lysates.

Chapter 5 – Conclusions and future perspectives

This study aimed to develop a specific fast and low-cost methodology to detect and quantify COMT protein by liquid chromatography-multiple reaction monitoring (MRM) mass spectrometry (LC/MS-MS).

Firstly, a COMT protein standard had to be produced, which was used in the creation, optimization and validation of the method. The approach used in the recombinant production of the SCOMT protein and its subsequent purification (by IMAC and SDS gel fractionation) showed to be profitable both in the level of amount of protein obtained, as in the economic level. However, this approach is time-consuming, which is why there was a very limited quantity of SCOMT standard.

A MRM method for the COMT measurement was developed and validated. Adjustable parameters, both source-dependent and scan-based parameters, were optimized. All the optimal parameters were found to be in the normal range. The validation performed follows the guidelines accepted internationally, evaluating selectivity, linearity, precision and accuracy, limit of detection and of quantification, carry-over and matrix effects. The current method proved to be selective for the analyte and compliant with a linear behaviour in the chosen range (25 - 200 μg mL^{-1}). The precision and accuracy were within accepted guidelines and the method showed no carry-over and matrix effect. Future work can be directed for the evaluation of the method on a more extensive range of concentrations in order to enhance the applicability of the method in a variety of samples. Furthermore, the calibration curve should incorporate three quality controls (QC) with high, medium and low concentrations, to help control the behaviour of the calibration curve. In this work, these improvements were not possible to be made due to the limitation of SCOMT standard and the available time.

Since the created method was applied to both isoforms of COMT, due to the chosen peptides for the analysis are common to both isoforms, the methodology applicability was evaluated through the analysis of cell lysates containing SCOMT or MBCOMT. However, later it should be also applied in analysis of COMT polymorphisms, such as Val/Met polymorphism. As future work, a method capable of distinguishing both isoforms in addition to their quantification should be considered. In addition, the method can be used for quantifying proteins in biological samples, such as erythrocytes.

In conclusion, the development of label-free quantitative method by LC/MS-MS has provided fast and low-cost measurement of COMT protein in complex samples, which is useful and suitable for the laboratory routine analysis. Moreover, the specific quantification of COMT

in biological samples may be useful to detect and control biochemical pathways of specific neurological diseases (PD, schizophrenia, obsessive-compulsive disorder) in which the protein is involved.

Chapter 6 - References

1. Axelrod J, Senoh S, Witkop B. 0-methylation of catechol amines in viva. J Biol Chem. 1958;233:697.
2. Chen J, Lipska BK, Halim N, Ma QD, Matsumoto M, Melhem S, et al. Functional analysis of genetic variation in catechol-O-methyltransferase (COMT): effects on mRNA, protein, and enzyme activity in postmortem human brain. The American Journal of Human Genetics. 2004;75(5):807-21.
3. Goodman JE, Lavigne JA, Wu K, Helzlsouer KJ, Strickland PT, Selhub J, et al. COMT genotype, micronutrients in the folate metabolic pathway and breast cancer risk. Carcinogenesis. 2001;22(10):1661-5.
4. Tenhunen J, Heikkilä P, Alanko A, Heinonen E, Akkila J, Ulmanen I. Soluble and membrane-bound catechol-O-methyltransferase in normal and malignant mammary gland. Cancer letters. 1999;144(1):75-84.
5. Lotta T, Vidgren J, Tilgmann C, Ulmanen I, Melen K, Julkunen I, et al. Kinetics of human soluble and membrane-bound catechol O-methyltransferase: a revised mechanism and description of the thermolabile variant of the enzyme. Biochemistry. 1995;34(13):4202-10.
6. Bai H-W, Shim J-Y, Yu J, Zhu BT. Biochemical and Molecular Modeling Studies of the O-Methylation of Various Endogenous and Exogenous Catechol Substrates Catalyzed by Recombinant Human Soluble and Membrane-Bound Catechol-O-Methyltransferases†. Chemical research in toxicology. 2007;20(10):1409-25.
7. Lundström K, Tenhunen J, Tilgmann C, Karhunen T, Panula P, Ulmanen I. Cloning, expression and structure of catechol-O-methyltransferase. Biochimica et Biophysica Acta (BBA)-Protein Structure and Molecular Enzymology. 1995;1251(1):1-10.
8. Huh M, Friedhoff AJ. Multiple molecular forms of catechol-O-methyltransferase. Evidence for two distinct forms, and their purification and physical characterization. Journal of Biological Chemistry. 1979;254(2):299-308.
9. Karayiorgou M, Altemus M, Galke BL, Goldman D, Murphy DL, Ott J, et al. Genotype determining low catechol-O-methyltransferase activity as a risk factor for obsessive-compulsive disorder. Proceedings of the National Academy of Sciences. 1997;94(9):4572-5.
10. Sweet R, Devlin B, Pollock B, Sukonick D, Kastango K, Bacanu S, et al. Catechol-O-methyltransferase haplotypes are associated with psychosis in Alzheimer disease. Molecular psychiatry. 2005;10(11):1026-36.
11. Harrison PJ, Tunbridge EM. Catechol-O-methyltransferase (COMT): a gene contributing to sex differences in brain function, and to sexual dimorphism in the predisposition to psychiatric disorders. Neuropsychopharmacology. 2008;33(13):3037-45.
12. Bonifácio MJ, Palma PN, Almeida L, Soares-da-Silva P. Catechol-O-methyltransferase and Its Inhibitors in Parkinson's Disease. CNS drug reviews. 2007;13(3):352-79.
13. Grossman MH, Szumlanski C, Littrell JB, Weinstein R, Weinshilboum RM. Electrophoretic analysis of low and high activity forms of catechol-O-methyltransferase in human erythrocytes. Life sciences. 1992;50(7):473-80.
14. Cotton NJ, Stoddard B, Parson WW. Oxidative inhibition of human soluble catechol-O-methyltransferase. Journal of Biological Chemistry. 2004;279(22):23710-8.
15. Tunbridge E, Bannerman D, Sharp T, Harrison P. Catechol-o-methyltransferase inhibition improves set-shifting performance and elevates stimulated dopamine release in the rat prefrontal cortex. The Journal of Neuroscience. 2004;24(23):5331-5.
16. Yavich L, Forsberg MM, Karayiorgou M, Gogos JA, Männistö PT. Site-specific role of catechol-O-methyltransferase in dopamine overflow within prefrontal cortex and dorsal striatum. The Journal of Neuroscience. 2007;27(38):10196-209.
17. Männistö PT, Kaakkola S. Catechol-O-methyltransferase (COMT): biochemistry, molecular biology, pharmacology, and clinical efficacy of the new selective COMT inhibitors. Pharmacological reviews. 1999;51(4):593-628.
18. Ellingson T, Duddempudi S, Greenberg BD, Hooper D, Eisenhofer G. Determination of differential activities of soluble and membrane-bound catechol-O-methyltransferase in tissues

and erythrocytes. Journal of Chromatography B: Biomedical Sciences and Applications. 1999;729(1):347-53.
19. Pedro AQ, Martins LM, Dias JM, Bonifácio MJ, Queiroz JA, Passarinha LA. An artificial neural network for membrane-bound catechol-O-methyltransferase biosynthesis with Pichia pastoris methanol-induced cultures. Microbial cell factories. 2015;14(1):1.
20. Min J.R. WH, Zeng H., Loppnau P., Sundstrom M., Arrowsmith C.H., Edwards A.M., Bochkarev A., Plotnikov A.N., Structural Genomics Consortium. The Crystal Structure of Human Catechol-O-methyltransferase domain containing 1 in complex with S-adenosyl-L-methionine. 2015.
21. Vidgren J, Svensson LA, Liljas A. Crystal structure of catechol O-methyltransferase. 1994.
22. Rutherford K, Le Trong I, Stenkamp R, Parson W. Crystal structures of human 108V and 108M catechol O-methyltransferase. Journal of molecular biology. 2008;380(1):120-30.
23. Bonifácio MJ, Archer M, Rodrigues ML, Matias PM, Learmonth DA, Carrondo MA, et al. Kinetics and crystal structure of catechol-o-methyltransferase complex with co-substrate and a novel inhibitor with potential therapeutic application. Molecular pharmacology. 2002;62(4):795-805.
24. Montag C, Jurkiewicz M, Reuter M. The role of the catechol-O-methyltransferase (COMT) gene in personality and related psychopathological disorders. CNS & Neurological Disorders-Drug Targets (Formerly Current Drug Targets-CNS & Neurological Disorders). 2012;11(3):236-50.
25. Tunbridge EM, Harrison PJ, Weinberger DR. Catechol-o-methyltransferase, cognition, and psychosis: Val 158 Met and beyond. Biological psychiatry. 2006;60(2):141-51.
26. Borroni B, Grassi M, Costanzi C, Zanetti M, Archetti S, Franzoni S, et al. Haplotypes in cathechol-O-methyltransferase gene confer increased risk for psychosis in Alzheimer disease. Neurobiology of Aging. 2007;28(8):1231-8.
27. Shield A, Thomae B, Eckloff B, Wieben ED, Weinshilboum RM. Human catechol O-methyltransferase genetic variation: gene resequencing and functional characterization of variant allozymes. Molecular psychiatry. 2004;9(2):151-60.
28. Witte AV, Flöel A. Effects of COMT polymorphisms on brain function and behavior in health and disease. Brain research bulletin. 2012;88(5):418-28.
29. Pedro A, Bonifacio M, Queiroz J, Maia C, Passarinha L. A novel prokaryotic expression system for biosynthesis of recombinant human membrane-bound catechol-O-methyltransferase. Journal of biotechnology. 2011;156(2):141-6.
30. Axelrod J, Tomchick R. Enzymatic O-methylation of epinephrine and other catechols. Journal of Biological Chemistry. 1958;233(3):702-5.
31. Flirski M, Sobow T, Kloszewska I. Behavioural genetics of Alzheimer's disease: a comprehensive review. Arch Med Sci. 2011;7:195-210.
32. Chakraborty C, Pal S, Doss CGP, Wen Z-H, Lin C-S. In silico analyses of COMT, an important signaling cascade of dopaminergic neurotransmission pathway, for drug development of Parkinson's disease. Applied biochemistry and biotechnology. 2012;167(4):845-60.
33. Assicot M, Bohuon C. Presence of two distinct catechol-O-methyltransferase activities in red blood cells. Biochimie. 1971;53(8):871-4.
34. Matsumoto M, Weickert CS, Akil M, Lipska B, Hyde T, Herman M, et al. Catechol O-methyltransferase mRNA expression in human and rat brain: evidence for a role in cortical neuronal function. Neuroscience. 2003;116(1):127-37.
35. Ulmanen I, Peränen J, Tenhunen J, Tilgmann C, Karhunen T, Panula P, et al. Expression and Intracellular Localization of Catechol O-methyltransferase in Transfected Mammalian Cells. European Journal of Biochemistry. 1997;243(1-2):452-9.
36. Chen C-H, Lee Y-R, Chung M-Y, Wei F-C, Koong F-J, Shaw C-K, et al. Systematic mutation analysis of the catechol O-methyltransferase gene as a candidate gene for schizophrenia. American Journal of Psychiatry. 1999;156(8):1273-5.
37. Wei J, Hemmings G. Lack of evidence for association between the COMT locus and schizophrenia. Psychiatric genetics. 1999;9(4):183-6.
38. Glatt SJ, Faraone SV, Tsuang MT. Association between a functional catechol O-methyltransferase gene polymorphism and schizophrenia: meta-analysis of case-control and family-based studies. American Journal of Psychiatry. 2003;160(3):469-76.
39. Fan J-B, Zhang C-S, Gu N-F, Li X-W, Sun W-W, Wang H-Y, et al. Catechol-O-methyltransferase gene Val/Met functional polymorphism and risk of schizophrenia: a large-scale association study plus meta-analysis. Biological psychiatry. 2005;57(2):139-44.

40. Strous RD, Bark N, Parsia SS, Volavka J, Lachman HM. Analysis of a functional catechol-O-methyltransferase gene polymorphism in schizophrenia: evidence for association with aggressive and antisocial behavior. Psychiatry research. 1997;69(2):71-7.
41. Lachman HM, Nolan KA, Mohr P, Saito T, Volavka J. Association between catechol O-methyltransferase genotype and violence in schizophrenia and schizoaffective disorder. American Journal of Psychiatry. 1998;155(6):835-7.
42. Shifman S, Bronstein M, Sternfeld M, Pisanté-Shalom A, Lev-Lehman E, Weizman A, et al. A highly significant association between a COMT haplotype and schizophrenia. The American Journal of Human Genetics. 2002;71(6):1296-302.
43. Gabrovsek M, Brecelj-Anderluh M, Bellodi L, Cellini E, Di Bella D, Estivill X, et al. Combined family trio and case-control analysis of the COMT Val158Met polymorphism in European patients with anorexia nervosa. American Journal of Medical Genetics Part B: Neuropsychiatric Genetics. 2004;124(1):68-72.
44. Borroni B, Grassi M, Agosti C, Costanzi C, Archetti S, Franzoni S, et al. Genetic correlates of behavioral endophenotypes in Alzheimer disease: role of COMT, 5-HTTLPR and APOE polymorphisms. Neurobiology of Aging. 2006;27(11):1595-603.
45. Hevir N, Šinkovec J, Rižner TL. Disturbed expression of phase I and phase II estrogen-metabolizing enzymes in endometrial cancer: lower levels of CYP1B1 and increased expression of S-COMT. Molecular and cellular endocrinology. 2011;331(1):158-67.
46. Bekris LM, Mata IF, Zabetian CP. The genetics of Parkinson disease. Journal of geriatric psychiatry and neurology. 2010;23(4):228-42.
47. Licker V, Kövari E, Hochstrasser DF, Burkhard PR. Proteomics in human Parkinson's disease research. Journal of proteomics. 2009;73(1):10-29.
48. Salat D, Tolosa E. Levodopa in the treatment of Parkinson's disease: current status and new developments. Journal of Parkinson's disease. 2013;3(3):255-69.
49. Malherbe P, Bertocci B, Caspers P, Zürcher G, Prada M. Expression of Functional Membrane-Bound and Soluble Catechol-O-Methyltransferase in Escherichia coli and a Mammalian Cell Line. Journal of neurochemistry. 1992;58(5):1782-9.
50. Tilgmann C, Melen K, Lundström K, Jalanko A, Julkunen I, Kalkkinen N, et al. Expression of recombinant soluble and membrane-bound catechol O-methyltransferase in eukaryotic cells and identification of the respective enzymes in rat brain. European Journal of Biochemistry. 1992;207(2):813-21.
51. Passarinha L, Bonifacio M, Queiroz J. Application of a fed-batch bioprocess for the heterologous production of hSCOMT in Escherichia coli. Journal of microbiology and biotechnology. 2009;19(9):972-81.
52. Dhanasekar L, Manikandan E. Analysis of Cladophora Glomerata in High Performance Liquid Chromatography-Mass Spectrometry (HPLC–MS).
53. Pedro AQ, Correia FF, Santos FM, Espírito-Santo G, Gonçalves AM, Bonifácio MJ, et al. Biosynthesis and purification of histidine-tagged human soluble catechol-O-methyltransferase. Journal of Chemical Technology and Biotechnology. 2016.
54. Cereghino GPL, Cereghino JL, Ilgen C, Cregg JM. Production of recombinant proteins in fermenter cultures of the yeast Pichia pastoris. Current opinion in biotechnology. 2002;13(4):329-32.
55. Gonçalves A, Pedro A, Maia C, Sousa F, Queiroz J, Passarinha L. Pichia pastoris: a recombinant microfactory for antibodies and human membrane proteins. J Microbiol Biotechnol. 2013;23(5):587-601.
56. Verma R, Boleti E, George A. Antibody engineering: comparison of bacterial, yeast, insect and mammalian expression systems. Journal of immunological methods. 1998;216(1):165-81.
57. Lundström K, Tilgmann C, Peränen J, Kalkkinen N, Ulmanen I. Expression of enzymatically active rat liver and human placental catechol-O-methyltransferase in Escherichia coli; purification and partial characterization of the enzyme. Biochimica et Biophysica Acta (BBA)-Gene Structure and Expression. 1992;1129(2):149-54.
58. Ball P, Knuppen R, Breuer H. Purification and Properties of a Catechol-O-Methyltransferase of Human Liver. European Journal of Biochemistry. 1971;21(4):517-25.
59. Correia F, Santos F, Pedro A, Bonifácio M, Queiroz J, Passarinha L. Recovery of biological active catechol-O-methyltransferase isoforms from Q-sepharose. Journal of separation science. 2014;37(1-2):20-9.

60. Tilgmann C, Ulmanen I. Purification methods of mammalian catechol-O-methyltransferases. Journal of Chromatography B: Biomedical Sciences and Applications. 1996;684(1):147-61.
61. White HL, Wu JC. Properties of catechol O-methyltransferases from brain and liver of rat and human. Biochemical Journal. 1975;145(2):135-43.
62. Nunes V, Bonifácio M, Queiroz J, Passarinha L. Assessment of COMT isolation by HIC using a dual salt system and low temperature. Biomedical Chromatography. 2010;24(8):858.
63. Pedro A, Pereira P, Bonifácio M, Queiroz J, Passarinha L. Purification of Membrane-Bound Catechol-O-Methyltransferase by Arginine-Affinity Chromatography. Chromatographia. 2015;78(21-22):1339-48.
64. Norrgran J, Williams TL, Woolfitt AR, Solano MI, Pirkle JL, Barr JR. Optimization of digestion parameters for protein quantification. Analytical biochemistry. 2009;393(1):48-55.
65. Noble JE, Bailey MJ. Quantitation of protein. Methods in enzymology. 2009;463:73-95.
66. Bradford MM. A rapid and sensitive method for the quantitation of microgram quantities of protein utilizing the principle of protein-dye binding. Analytical biochemistry. 1976;72(1-2):248-54.
67. Smith PK, Krohn RI, Hermanson G, Mallia A, Gartner F, Provenzano M, et al. Measurement of protein using bicinchoninic acid. Analytical biochemistry. 1985;150(1):76-85.
68. Lowry OH, Rosebrough NJ, Farr AL, Randall RJ. Protein measurement with the Folin phenol reagent. J biol Chem. 1951;193(1):265-75.
69. Collier TS, Muddiman DC. Analytical strategies for the global quantification of intact proteins. Amino acids. 2012;43(3):1109-17.
70. Rauh M. LC–MS/MS for protein and peptide quantification in clinical chemistry. Journal of Chromatography B. 2012;883:59-67.
71. Lilley KS, Friedman DB. All about DIGE: quantification technology for differential-display 2D-gel proteomics. Expert review of proteomics. 2004;1(4):401-9.
72. Brewis IA, Brennan P. Proteomics technologies for the global identification and quantification of proteins. Adv Protein Chem Struct Biol. 2010;80(15):1-44.
73. Aebersold R, Mann M. Mass spectrometry-based proteomics. Nature. 2003;422(6928):198-207.
74. James A, Jorgensen C. Basic design of MRM assays for peptide quantification. LC-MS/MS in Proteomics: Methods and Applications. 2010:167-85.
75. Westermeier R, Naven T, Höpker H-R. Proteomics in practice: a guide to successful experimental design: John Wiley & Sons; 2008.
76. Jennings KR. The changing impact of the collision-induced decomposition of ions on mass spectrometry. International Journal of Mass Spectrometry. 2000;200(1):479-93.
77. Vaudel M, Sickmann A, Martens L. Peptide and protein quantification: a map of the minefield. Proteomics. 2010;10(4):650-70.
78. Bantscheff M, Schirle M, Sweetman G, Rick J, Kuster B. Quantitative mass spectrometry in proteomics: a critical review. Analytical and bioanalytical chemistry. 2007;389(4):1017-31.
79. Agger SA, Marney LC, Hoofnagle AN. Simultaneous quantification of apolipoprotein AI and apolipoprotein B by liquid-chromatography–multiple-reaction–monitoring mass spectrometry. Clinical Chemistry. 2010;56(12):1804-13.
80. Van Eeckhaut A, Lanckmans K, Sarre S, Smolders I, Michotte Y. Validation of bioanalytical LC–MS/MS assays: evaluation of matrix effects. Journal of Chromatography B. 2009;877(23):2198-207.
81. Schmidt A, Picotti P, Aebersold R. Proteomanalyse und Systembiologie. Biospektrum. 2008;14(1):44.
82. Jin J, Min H, Kim SJ, Oh S, Kim K, Yu HG, et al. Development of Diagnostic Biomarkers for Detecting Diabetic Retinopathy at Early Stages Using Quantitative Proteomics. Journal of diabetes research. 2015;2016.
83. Kuzyk MA, Parker CE, Domanski D, Borchers CH. Development of MRM-based assays for the absolute quantitation of plasma proteins. The Low Molecular Weight Proteome: Methods and Protocols. 2013:53-82.
84. Mermelekas G, Vlahou A, Zoidakis J. SRM/MRM targeted proteomics as a tool for biomarker validation and absolute quantification in human urine. Expert review of molecular diagnostics. 2015;15(11):1441-54.
85. MacLean B, Tomazela DM, Shulman N, Chambers M, Finney GL, Frewen B, et al. Skyline: an open source document editor for creating and analyzing targeted proteomics experiments. Bioinformatics. 2010;26(7):966-8.

86. Laemmli UK. Cleavage of structural proteins during the assembly of the head of bacteriophage T4. nature. 1970;227:680-5.
87. Passarinha L, Bonifacio M, Queiroz J. Comparative study on the interaction of recombinant human soluble catechol-O-methyltransferase on some hydrophobic adsorbents. Biomedical Chromatography. 2007;21(4):430-8.
88. Shevchenko A, Tomas H, Havli J, Olsen JV, Mann M. In-gel digestion for mass spectrometric characterization of proteins and proteomes. Nature protocols. 2006;1(6):2856-60.
89. Medzihradszky KF. In-Solution Digestion of Proteins for Mass Spectrometry. Methods in enzymology. 2005;405:50-65.
90. UniProt. 2016. Available from: http://www.uniprot.org/blast/uniprot/B201610078A530B6CA0138AFAA6D2B97CE8C2A924B0924ER. (retrieved at 27/04/2016)
91. Software ML. Skyline. 3.5 ed. Available from: https://skyline.gs.washington.edu/labkey/project/home/software/Skyline/begin.view (retrieved at 24/04/2016)
92. Röst H. SRM Collider. 1.4 ed. 2012. Available from: http://www.srmcollider.org/srmcollider/srmcollider.py (retrieved at 30/04/2016)
93. Chen T, Chen Z, Zhang S, Zhang K, Wang L. Development and validation of a LC–MS/MS method for quantification of hetrombopag for pharmacokinetics study. SpringerPlus. 2015;4(1):1.
94. Kay RG, Gregory B, Grace PB, Pleasance S. The application of ultra-performance liquid chromatography/tandem mass spectrometry to the detection and quantitation of apolipoproteins in human serum. Rapid communications in mass spectrometry. 2007;21(16):2585-93.
95. Boehm AM, Pütz S, Altenhöfer D, Sickmann A, Falk M. Precise protein quantification based on peptide quantification using iTRAQ™. Bmc Bioinformatics. 2007;8(1):1.
96. Röst H, Malmström L, Aebersold R. A computational tool to detect and avoid redundancy in selected reaction monitoring. Molecular & Cellular Proteomics. 2012;11(8):540-9.
97. FDA C. Guidance for industry: bioanalytical method validation. US Department of Health and Human Services. Food and Drug Administration, Center for Drug Evaluation and Research (CDER), Center for Veterinary Medicine (CV). 2001. Available from: http://www.fda.gov/downloads/Drugs/Guidance/ucm070107.pdf (retrieved at 28/08/2016)
98. Guideline IHT. Validation of analytical procedures: text and methodology. Q2 (R1). 2005;1. Available from: http://www.ich.org/fileadmin/Public_Web_Site/ICH_Products/Guidelines/Quality/Q2_R1/Step4/Q2_R1__Guideline.pdf (retrieved at 28/08/2016)
99. WADA. Minimum criteria for chromatographic-mass spectrometric confirmation of the identity of analytes for doping control purposes. 2015; Available from: https://wada-main-prod.s3.amazonaws.com/resources/files/wada_td2015idcr_minimum_criteria_chromato-mass_spectro_conf_en.pdf. (retrieved at 28/08/2016)
100. Wille SM, Peters FT, Di Fazio V, Samyn N. Practical aspects concerning validation and quality control for forensic and clinical bioanalytical quantitative methods. Accreditation and quality assurance. 2011;16(6):279-92.
101. Araujo P. Key aspects of analytical method validation and linearity evaluation. Journal of chromatography B. 2009;877(23):2224-34.